https://doi.org/10.5194/bg-2021-230
Preprint. Discussion started: 18 October 2021

Biogeosciences Discussions Open Access EGU

Late Neogene evolution of modern deep-dwelling plankton

Flavia Boscolo-Galazzo[1‡*], Amy Jones[2], Tom Dunkley Jones[2], Katherine A. Crichton[1⸸], Bridget S. Wade[3], Paul N. Pearson[1]

[1]Cardiff University, School of Earth and Environmental Sciences, Cardiff (UK).

[2]Birmingham University, School of Geography, Earth and Environmental Sciences, Birmingham (UK).

[3]University College London, Department of Earth Sciences, London (UK).

‡Now at Bergen University, Department of Earth Science and Bjerknes Center for Climate Research, Bergen (Norway).

⸸Now at Exeter University, Department of Geography, Exeter (UK)

*corresponding author: flavia.boscologalazzo@uib.no

The fossil record of marine microplankton provides insights into the evolutionary drivers which led to the origin of modern deep-water plankton, one of the largest component of ocean biomass. We use global abundance and biogeographic data combined with depth habitat reconstructions to determine the environmental mechanisms behind speciation in two groups of pelagic microfossils over the past 15 million years. We compare our microfossil datasets with water column profiles simulated in an Earth System model. We show that deep-living planktonic foraminiferal (zooplankton) and calcareous nannofossil (mixotroph phytoplankton) species were virtually absent globally during the peak of the middle Miocene warmth. Evolution of deep-dwelling planktonic foraminifera started from subpolar-midlatitude species during late Miocene cooling, via allopatry. Deep-dwelling species subsequently spread towards lower latitudes and further diversified via depth sympatry, establishing modern communities stratified hundreds of meters down the water column. Similarly, sub-euphotic zone specialist calcareous nannofossils become a major component of tropical and sub-tropical assemblages during the latest Miocene to early Pliocene. Our model simulations suggest that increased organic matter and oxygen availability for

https://doi.org/10.5194/bg-2021-230
Preprint. Discussion started: 18 October 2021

planktonic foraminifera, and increased nutrients and light penetration for nannoplankton, favored the evolution of new deep water niches. These conditions resulted from global cooling and the associated increase in the efficiency of the biological pump over the last 15 million years.

1. Introduction

The biodiversity of planktonic and nektonic organisms is difficult to explain given the uniform character and vastness of pelagic environments, where genetic isolation seems difficult to maintain (Norris, 2000). Planktonic microorganisms with mineralized shells have often been used as a model to study the mode and tempo of species origination in the open ocean, due to the abundance, widespread distribution, and temporal continuity of their fossil record (e.g., Pearson et al., 1997; Norris, 2000; Bown et al., 2004; Ezard et al., 2011; Norris et al., 2013). Because of the great fossilization potential of their calcium carbonate tests across much of the global ocean, their relatively simple and well-established taxonomy, and highly resolved biostratigraphy, planktonic foraminifera and calcareous nannofossils are amongst the best studied fossil groups. Planktonic foraminifera are heterotrophic zooplankton, with different species specialized to feed on different types of food, from other plankton to sinking detritus. In the modern ocean, planktonic foraminifera live stratified across a range of depths spanning from the surface to hundreds of meters down the water column (Rebotim et al., 2017; Meilland et al., 2019). Properties such as food quantity and quality, oxygen, light and pressure all change markedly across the first few hundreds of meters of the ocean. Depending on such down-column variability in environmental conditions, planktonic foraminifera can actively control their living depth of preference, which remains relatively stable during their adult life-stage (Hull et al., 2011; Weiner et al., 2012; Rebotim et al., 2017; Meilland et al., 2019; Duan et al., 2021). A key advantage of using planktonic

https://doi.org/10.5194/bg-2021-230
Preprint. Discussion started: 18 October 2021

foraminifera for evolutionary studies is the ability to extract ecological information from their shell chemistry. This provides invaluable information about species-specific functional ecology (e.g., feeding strategy) and habitat preferences (e.g., surface versus deep waters), which in combination with biogeographic, taxonomic, biometric, and stratigraphic data have often been used to infer speciation and extinction mechanisms (Norris et al., 1993; Norris et al., 1994; Pearson et al., 1997; Hull and Norris, 2009; Pearson and Coxall, 2012; Woodhouse et al., 2021) and reconstruct phylogeny (Aze et al., 2011).

Calcareous nannoplankton also have a highly resolved and continuous fossil record; they are the most abundant microfossils in oceanic pelagic sediments, and similar to planktonic foraminifera, their spatial distribution ranges from tropical to subpolar latitudes (Poulton et al. 2017). In the modern ocean they also live stratified in the water column, with species adapted to euphotic waters, and species adapted to live deeper (Poulton et al., 2017). In contrast to planktonic foraminifera, nannoplankton are predominantly autotrophic, performing photosynthesis in water where light penetration is sufficient, although there is evidence for heterotrophy (mixotrophic behavior) in some extant (Godrjian et al., 2020) and fossil (Gibbs et al., 2020) species. In euphotic waters, organic matter production from nannoplankton is at the base of pelagic food chains and of the functioning of the ocean biological carbon pump. Taxonomic, biometric and stratigraphic data have been used to establish phylogenetic relationships between fossil nannoplankton species (Young and Bown, 1997).

Little emphasis has been given to the long-term drivers of evolutionary patterns observed in fossil plankton from species to phylum level, although more recently, a broad connection with changing climate and ocean properties has been suggested (e.g., Ezard et al., 2011; Norris et al., 2013; Frass et al., 2015; Henderiks et al., 2020; Lowery et al., 2020). Boscolo-Galazzo, Crichton

https://doi.org/10.5194/bg-2021-230
Preprint. Discussion started: 18 October 2021

et al. (2021) showed that over the last 15 million years the remineralization of particulate organic carbon (POC) in surface waters declined markedly driven by climate and ocean cooling (Kennett and Von der Borch, 1985; Kennett and Exon, 2004; Cramer et al., 2011; Zhang et al., 2014; Herbert et al., 2016; Sosdian et al., 2018; Super et al., 2020), increasing the efficiency of the ocean biological pump in delivering organic matter at depth. Such a mechanism was key to promote the evolution of life in deep waters, allowing the development of the modern twilight zone ecosystem (Boscolo-Galazzo, Crichton et al., 2021). The goal of this study is to combine the fossil record of two ecologically complementary calcareous microplankton groups seldom analyzed together, planktonic foraminifera and nannoplankton, and together with model simulations, help disentangle the evolutionary drivers of modern deep-dwelling plankton. We use the planktonic foraminiferal dataset from Boscolo-Galazzo, Crichton et al. (2021) and extend our analysis to calcareous nannofossils in coeval sediment samples to assess their abundance and distribution pattern. We compare the results from these two groups and contrast them against time and site-specific model water column profiles for POC and oxygen (O_2) obtained from the cGENIE Earth System model. Further, using stable isotopes, depth habitat reconstructions, abundance and biogeography data we reconstruct the speciation mechanisms which led to the evolution of modern deep-dwelling planktonic foraminiferal species.

2. Methods

2.1 Planktonic foraminifera

In this study we focus on the deep-dwelling groups of macroperforate planktonic foraminifera of the hirsutellids, globorotaliids, truncorotaliids and globoconellids, which in the modern ocean calcify and live mostly in the twilight zone of the ocean, i.e. between 200-1000 m (Birch et al.,

https://doi.org/10.5194/bg-2021-230
Preprint. Discussion started: 18 October 2021

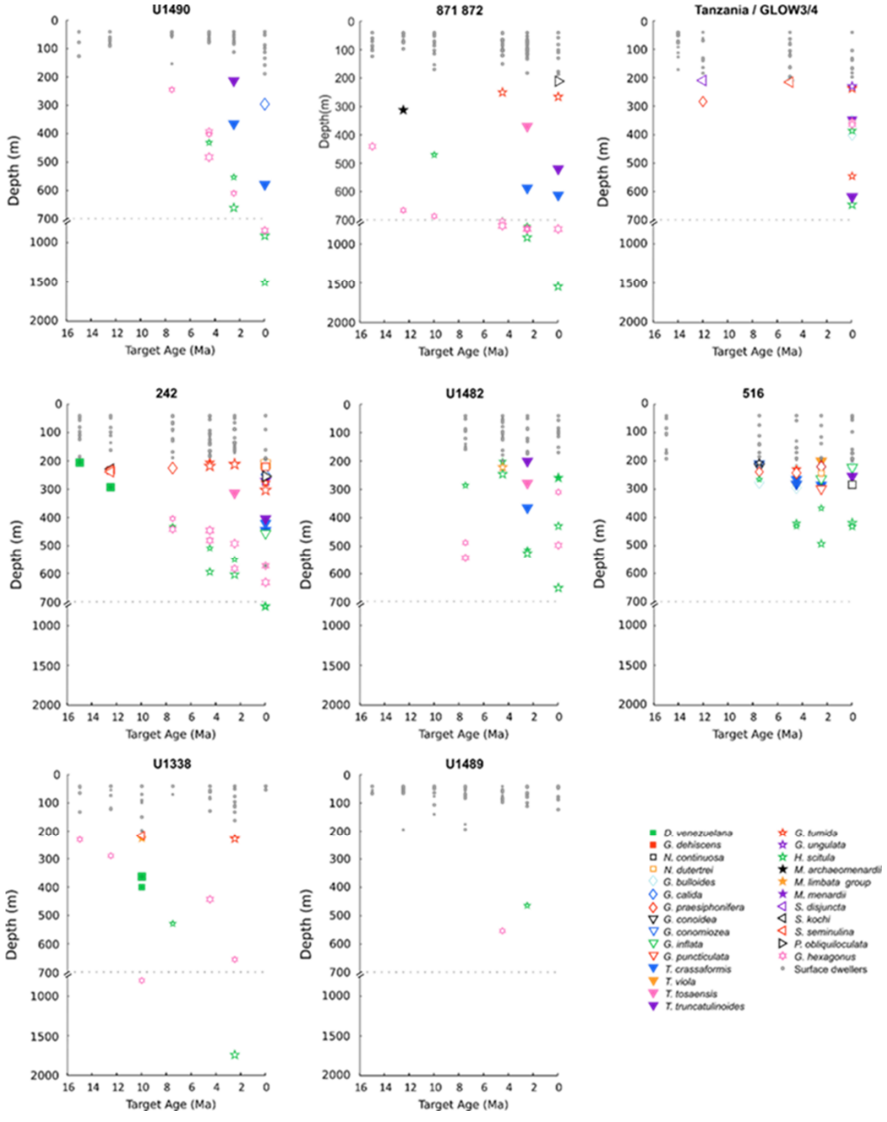

Figure 1. Depth-habitat reconstructions for middle Miocene to present planktonic foraminiferal species at the investigated sites. Surface dwellers (species living at depths shallower than 200 m) are indicated with a grey dot, deeper species are indicated with colored symbols. Relative size of symbols represents the size fractions of the sample. Reproduced from Boscolo-Galazzo, Crichton et al. (2021).

https://doi.org/10.5194/bg-2021-230
Preprint. Discussion started: 18 October 2021

2012; Rebotim et al., 2017), and have a more complete fossil record than deep-dwelling microperforate planktonic foraminifera (Kennett and Srinivasan, 1983).

Planktonic foraminiferal data and depth habitat reconstructions (Fig. 1) are from Boscolo-Galazzo, Crichton et al. (2021). They were obtained from globally and latitudinally distributed DSDP/ODP/IODP sites and from cores drilled onshore and offshore Tanzania, all characterized by abundant calcareous microfossils (Boscolo-Galazzo, Crichton et al., 2021). The work was focused on seven target ages (15 Ma, 12.5 Ma, 10 Ma, 7.5 Ma, 4.5 Ma, 2.5 Ma, 0 Ma/Holocene). To avoid sample-aliasing, bulk sediment stable isotopes were measured on an average of ten samples per target age at each site. The sample displaying mean oxygen stable isotope values was chosen for subsequent analyses (Boscolo-Galazzo, Crichton et al., 2021). Ages were determined based on biostratigraphic analysis mostly following the biozonation scheme by Wade et al. (2011).

Foraminiferal picking for stable isotope measurements were conducted from the size fractions: 180-250 μm, 250-300 μm, 300-355 μm (Boscolo-Galazzo, Crichton et al., 2021). Stable isotopes were measured on an average of 15 different species per sample, using ~25 specimens for common species, and as many specimens as possible for rare species. Stable isotopes were measured at Cardiff University. Stable isotope results are shown in Figs. S1 to S9 in the Supplement. Only data from the largest of the three measured size fractions are shown when data from more than one size fraction are available. Data from size fractions other than those above are shown only when a species did not occur within the preferred size interval. Foraminiferal abundance counts were carried out in two size fractions, 180-250 μm and >250 μm, counting up to 300 specimens in each. Total abundances were derived by summing up abundances from these two size fractions.

Boscolo-Galazzo, Crichton et al. (2021) reconstructed planktonic foraminiferal depth habitat (Fig. 1) using a combined model-data approach, solving the paleotemperature equation of Kim and

https://doi.org/10.5194/bg-2021-230
Preprint. Discussion started: 18 October 2021

126 O'Neill (1997) for each data point using measured foraminiferal $\delta^{18}O$, global ice volume estimates,
127 and the cGENIE modeled salinity field to determine local water $\delta^{18}O$, and then use the model
128 temperature-depth curve to determine depth. The full method is described in Boscolo-Galazzo,
129 Crichton et al. (2021).
130
131 **2.2 Calcareous Nannofossils**
132 Quantitative calcareous nannofossil data were collected from the same samples as used for
133 planktonic foraminiferal analysis or, when this was not possible, stratigraphically adjacent samples
134 (Table S1 in the Supplement). A cascading count technique was used to maximise nannofossil
135 diversity recovery and quantification of low abundance species (Styzen, 1997). Nannofossils were
136 counted per field of view (FOV) until a minimum of 400 specimens were achieved for each sample.
137 However, if a high abundance species exceeded an average of 25 specimens per FOV, it was
138 excluded from subsequent counts in that sample and its abundance scaled-up based on its average
139 abundance and the total numbers of FOV counted. Only specimens directly counted contributed
140 to the minimum count threshold of 400 specimens. An additional scan of two slide transects were
141 undertaken to record rare species not observed during the extended count and are included in the
142 total species richness and diversity analyses. Samples for nannofossil analysis were prepared using
143 the smear slide technique (Bown & Young, 1998). Calcareous nannofossils were observed using
144 both plane-polarised (PPL) and cross-polarised light (XPL) on a Zeiss Axioscope light-microscope
145 at x1000 magnification. Identification and taxonomy used herein follows Young et al. (1997) and
146 is coherent with the recent Neogene calcareous nannofossil taxonomy (Ciummelli et al., 2016;
147 Bergen et al., 2017; Blair et al., 2017; Boesiger et al., 2017; Browning et al., 2017; de Kaenel et
148 al., 2017).

https://doi.org/10.5194/bg-2021-230
Preprint. Discussion started: 18 October 2021

149 **2.3 Plankton Ecogroups**

150 In order to compare the datasets obtained from the planktonic foraminiferal and nannofossil
151 analysis, we grouped species into ecogroups based on depth-habitat preferences. Planktonic
152 foraminiferal ecogroups are defined based on paleodepth habitat reconstructions from Boscolo-
153 Galazzo, Crichton et al. (2021): the euphotic zone ecogroups includes species with an average
154 depth habitat shallower than 200 m (the bottom of the euphotic zone), the twilight zone ecogroup
155 includes species with an average depth habitat coinciding with the twilight zone (200-1000 m).
156 The twilight zone ecogroup is largely composed of species within the globoconellids, the
157 *Globorotalia merotumida-tumida* lineage, the hirsutellids and the truncorotaliids, but also includes
158 species from other genera, such as *Globigerinella calida*, *Globorotaloides hexagonus*, *G.*
159 *variabilis*, and *Pulleniatina obliquiloculata*. *Dentoglobigerina venezuelana* has a changeable
160 depth habitat through time (see discussion in Wade et al., 2018); following the depth habitat
161 reconstructions from Boscolo-Galazzo, Crichton et al., (2021) it was grouped as euphotic zone
162 species for target ages 15, 12.5, 7.5, 4.5 Ma and as twilight zone species for target age 10 Ma.
163 Species were excluded from the grouping when they are known to have a marked seasonality in
164 abundance and depth habitat (*Globigerina bulloides*, *Globigerinella praesiphonifera* and the
165 neogloboquadrinids) (e.g., Jonkers and Kucera, 2015; Greco et al., 2019), and if they were too rare
166 and depth habitat reconstruction was not possible (*Candeina nitida*).

167 Three ecogroups for calcareous nannofossils are used: upper-euphotic, lower-euphotic and
168 sub-euphotic. The upper-euphotic group is represented by: *Discoaster* spp., *Rhabdosphaera*
169 *xiphos*, *Reticulofenestra* spp. and *Gephyrocapsa* spp. (excluding *G. ericsonii*); the lower-euphotic
170 ecogroup contains: *Rhabdosphaera clavigera*, *Gephyrocapsa ericsonii* and *Ceratolithus* spp.,
171 finally the subeuphotic ecogroup includes: *Florisphaera profunda* and *Calciosolena murrayi*.

https://doi.org/10.5194/bg-2021-230
Preprint. Discussion started: 18 October 2021

Because species specific stable isotope measurements and depth habitat reconstructions are difficult for calcareous nannofossils, species depth-habitat preference was assigned based on the literature (Poulton et al., 2017; Tangunan et al., 2018). In particular, Poulton et al. (2017) described vertically separated coccolithophores communities sampled during a meridional cruise in the Atlantic Ocean. Here we use their criteria for assigning nannofossil species into ecogroups, whereby in the upper-euphotic zone ecogroup we include species found to live in waters with >10% surface irradiance, in the lower-euphotic zone ecogroup we group species found to live in waters with 10-1% irradiance, and in the sub-euphotic zone ecogroup we group species found to live in waters with <1%, i.e. too low to support photosynthesis (Poulton et al., 2017). *Discoaster* become extinct in the early Pleistocene, therefore, its depth habitat remains under debate as the group has no extant relative (Schueth and Bralower, 2015; Tangunan et al., 2018). However, geochemical evidence from oxygen isotope values of *Discoaster* and planktonic foraminifera (*Globorotalia menardii*, *Dentoglobigerina altispira* and *Globigerinoides obliquus*), reveal comparable values and signifies that *Discoaster* likely inhabited the upper euphotic zone (Minoletti et al., 2001).

For each target age, the relative abundance of ecogroups was calculated summing up the abundance counts of all the individual species pertaining to an ecogroup at each site, hence, ecogroup abundance data represent global mean values. For both nannofossils and planktonic foraminifera, the percentage of each ecogroup per time bin was converted into pie-charts (Figs. 2-5). Diversity indexes for both foraminiferal and nannofossil ecogroup were calculated using the statistical software Past (Hammer et al., 2001) (Fig. 6).

https://doi.org/10.5194/bg-2021-230
Preprint. Discussion started: 18 October 2021

Biogeosciences Discussions Open Access EGU

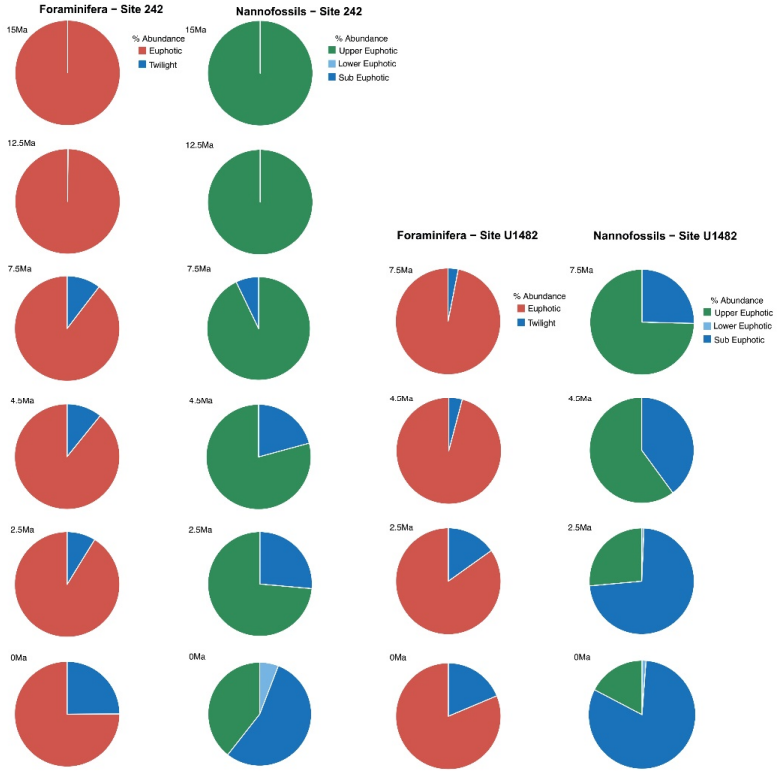

194

195 **Figure 2.** Foraminiferal and nannofossil ecogroup abundance at Site 242 and U1482.

196

197

198

199

200

201

202

203

204

https://doi.org/10.5194/bg-2021-230
Preprint. Discussion started: 18 October 2021

205 **2.4 cGENIE model**

206 We extracted model output for Particulate Organic Carbon (POC) and oxygen concentration
207 from the cGENIE simulations for each of the seven target ages as described fully in Boscolo-
208 Galazzo, Crichton et al. (2021). To facilitate a general discussion of near-surface changes, we
209 divided the data latitudinally by calculating the arithmetic mean for low latitudes (<16° latitude),
210 two mid-latitude bands (mid 1: 16° to 40°, mid 2: 40° to 56°) and high latitudes (>56°). The
211 cGENIE simulations take account of changing boundary conditions including CO_2 forcing,
212 bathymetry and ocean circulation (Crichton et al., 2020). The model's ocean biological carbon
213 pump is temperature dependent, where temperature affects both nutrient uptake rates at the surface
214 and remineralization rates of sinking particulate organic matter down the water column (Crichton
215 et al., 2021).

216 **3. Results**

217 **3.1 Plankton Ecogroups**

218 For both calcareous nannoplankton and planktonic foraminifera, the variation in abundance
219 of euphotic zone and deeper-dwelling ecogroups show global patterns recognised across sites.
220 Additionally both group indicate a long-term directionality towards increased abundance of deep-
221 dwelling ecotypes. Among planktonic foraminifera, the twilight zone ecogroup increases in
222 abundance through time starting at 7.5 Ma (Fig. 6). The relative abundance of the twilight zone
223 ecogroup in the middle Miocene is 15% and it increases to ~30% in the Holocene time slice (Fig.
224 6). The average abundance of the euphotic zone species ecogroup in the middle Miocene is 85%
225 and it decreases through time until reaching 60% in the Holocene (Fig. 6). In the twilight zone
226 ecogroup we observe an increase in the total number of species from about 1-2 species at 15 Ma,
227 to 14 species in the Holocene (Fig. 6). In the middle Miocene this group comprised 1/6 of the total

https://doi.org/10.5194/bg-2021-230
Preprint. Discussion started: 18 October 2021

number of species in our samples, while in the Holocene it represents almost the half. All the diversity indexes show a late Miocene to Holocene increasing trend for the twilight zone ecogroup (Fig. 6).

Calcareous nannofossil assemblages are dominated by the upper-euphotic ecogroup from 15 to 10 Ma at all sites (Figs. 2-5). At 7.5 Ma the sub-euphotic ecogroup first becomes a significant component of assemblages at Indian Ocean sub-tropical Sites U1482 and to some extent Site 242, but it is not until the 4.5 Ma time slice that the sub-euphotic ecogroup becomes a significant component of assemblages at the majority of locations (Sites 516, 871/872, 242, U1338, U1482, U1489; Figs. 2-5). By the Holocene time slice, coccoliths of sub-euphotic species are dominant at most locations, except at Eastern Equatorial Pacific Site U1338 (Figs. 6 and 4). At the southern high latitude Site 1138 there is no significant contribution from coccoliths of either lower-euphotic or sub-euphotic species at any point, although there is no data from the Pliocene to Holocene time slices at this location (Fig. 5). Global average compositions of calcareous nannofossil assemblages reflect the changes noted above, with a marked and rapid decline in the relative contribution of the upper-euphotic ecogroup, and a corresponding increase in the sub-euphotic zone ecogroup through the Pliocene and to Holocene (Fig. 6).

3.2 Planktonic foraminiferal deep-dwelling species: depth habitat, abundance and biogeography

3.2.1 Hirsutellids

The only hirsutellid species occurring in our Miocene samples is *Hirsutella scitula*. At 15 Ma this morphospecies is common only at Site 1138 (~8%), sporadically occurs at Site 516 (<1%) and is absent at the other investigated sites (Figs. 7). Oxygen isotopes range from 0.5 to 1.3‰ (Figs. S1-

https://doi.org/10.5194/bg-2021-230
Preprint. Discussion started: 18 October 2021

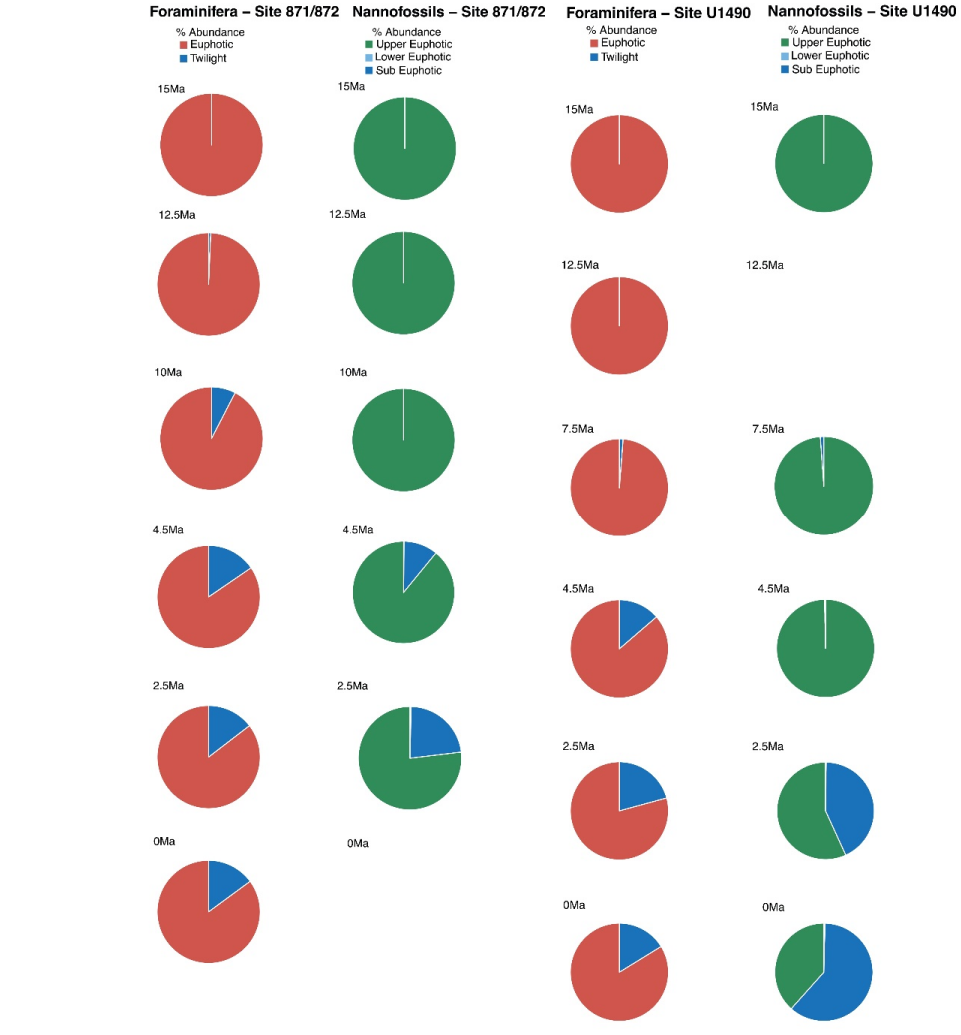

Figure 3. Foraminiferal and nannofossil ecogroup abundance at Site 871/872 and U1490.

https://doi.org/10.5194/bg-2021-230
Preprint. Discussion started: 18 October 2021

S2). Depth-habitat reconstructions for Site 1138 are unattainable from $\delta^{18}O$ data due to the overprinting effect of subpolar front shifts at this location, but habitat reconstruction at Site 516 suggests a paleodepth habitat shallower than 200 m. By 12.5 Ma, *H. scitula* appears at Site U1338 and U1489 in very low abundance (<0.5%) (Fig. 7). At Site U1489 the species was so rare that it was encountered when picking for stable isotopes and no more when counting for species abundances, despite the use of different splits of the residue. No differences were observed between 12.5 and 10 Ma in the biogeography of *H. scitula* (Fig. 7). However, by 7.5 Ma, *H. scitula* occurs at all our low latitude sites (Fig. 8) with oxygen isotopes ranging from -0.5 to 2.0‰ (Figs. S3-S9), which according to depth habitat reconstructions translates to 250 and 500 m water depth (Boscolo-Galazzo, Crichton et al., 2021). This is similar to that of *Globorotaloides hexagonus* (Fig. 1), the only twilight zone dweller we observed at tropical sites at 15 Ma, displaying stable isotopes ranging from 0 to 1‰, which translates to depths around 300-500 m. In the late middle Miocene the stable isotope values of *G. hexagonus* increase to 2-2.5‰ (Figs. S3-S9). Similarly, the oxygen isotope values of tropical *H. scitula* increased through time, reaching 2-3‰ in the youngest target ages. In line with this, the reconstructed depth habitat of *H. scitula* and *G. hexagonus* increases through time in a stepwise fashion, and in the Holocene it reaches down to 800-1500 m (Fig. 1) (Boscolo-Galazzo, Crichton et al., 2021). *Hirsutella scitula* becomes gradually more common at low latitude sites through the Miocene-Pliocene, although it never becomes abundant. In our record, *Hirsutella margaritae* and *H. theyeri* first appear in the early Pliocene at a depth between 200-300 m (Fig. 1) (oxygen isotopes range -1 to -0.5‰), similar to that of *H. hirsuta* (oxygen isotopes range 0 to 1‰) when it first appears in the Holocene (Figs. S3-S9).

https://doi.org/10.5194/bg-2021-230
Preprint. Discussion started: 18 October 2021

Biogeosciences Discussions Open Access EGU

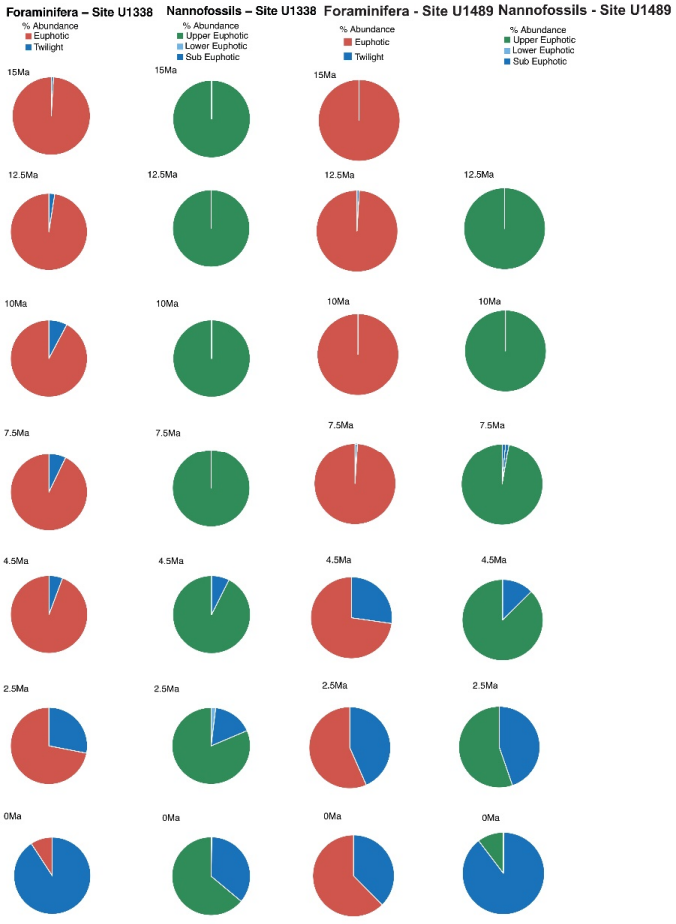

Figure 4. Foraminiferal and nannofossil ecogroup abundance at Site U1338 and U1489.

https://doi.org/10.5194/bg-2021-230
Preprint. Discussion started: 18 October 2021

294 **3.2.2 Truncorotaliids**

295 The earliest appearances of *Truncorotalia crassaformis* in our record corresponds to our 4.5 Ma
296 time slice at Site 1138 in the Indian Ocean sector of the Southern Ocean where it represents >20%
297 of the assemblage, and in coeval sediments at mid-latitude Site 516 in the southwest Atlantic,
298 where it represents ~9% of the assemblage (Fig. 9), with oxygen isotopes ranging from 1.5 to 3.0‰
299 (Figs. S1-S2). At Site 516 we observe the co-occurrence of *T. oceanica* (~14%) and *T.*
300 *crassaformis* in the early Pliocene, and of *T. viola* (~5%) and *T. crassaformis* (~13%) in the late
301 Pliocene (Fig. 10). We did not observe *T. oceanica* and *T. viola* anywhere else. *T. oceanica* and *T.*
302 *crassaformis* display almost overlapping $\delta^{18}O$ values and depth habitat (Fig. S2) but *T.*
303 *crassaformis* has 0.5‰ lower $\delta^{13}C$ values. Oxygen stable isotope data (1‰; Fig. S2) and habitat
304 reconstructions for Site 516 indicate that a subsurface habitat (>200 m) was already occupied by
305 *T. crassaformis* at the beginning of its evolutionary history (Fig. 1). The late Pliocene appearance
306 of *T. viola* at Site 516, which differs from *T. crassaformis* in having a more convex umbilical side,
307 a triangular outline and a subacute profile, is associated with a shift to more positive oxygen
308 isotope values of *T. crassaformis* (1.5‰) and to slightly greater depths (Fig. 1).

309 We find *T. crassaformis* by the late Pliocene at our investigated tropical and subtropical
310 sites (Figs. 10-11), with oxygen isotope values ranging from 1.0 to 2.0‰ which translate to depth
311 habitats of 400-600 m (Boscolo-Galazzo, Crichton et al., 2021; Fig.1). The appearance of *T.*
312 *crassaformis* at our low latitude sites is coeval with the appearance in our record of *Truncorotalia*
313 *tosaensis*, morphologically transitional between *T. crassaformis* and *T. truncatulinoides* (Lazarus
314 et al., 1995) (Fig. 10). *Truncorotalia tosaensis* displays oxygen isotopes values ranging from 0 to
315 0.5‰ (Figs. S1-S9), which translate to 300-350 m depth (Fig. 1). Consistent with earlier findings
316 (Lazarus et al., 1995), we record the first occurrence of *T. truncatulinoides* in the late Pliocene in

https://doi.org/10.5194/bg-2021-230
Preprint. Discussion started: 18 October 2021

317 the south-west Pacific (Site U1482), and only later in the North Pacific (Site 872), Indian Ocean
318 (Site 242) and South Atlantic (Site 516) (Fig. 11). *Truncorotalia truncatulinoides* records oxygen
319 isotope values ranging from -1 to 2‰, more negative than coeval *T. crassaformis* (Figs. S3-S9).
320 *Truncorotalia truncatulinoides*, although reported in the modern tropical ocean as one of the
321 species living at the greatest depths, occupies a shallower depth habitat than *T. crassaformis* when
322 it first appears in our tropical to subtropical records (2.5 Ma).
323

https://doi.org/10.5194/bg-2021-230
Preprint. Discussion started: 18 October 2021

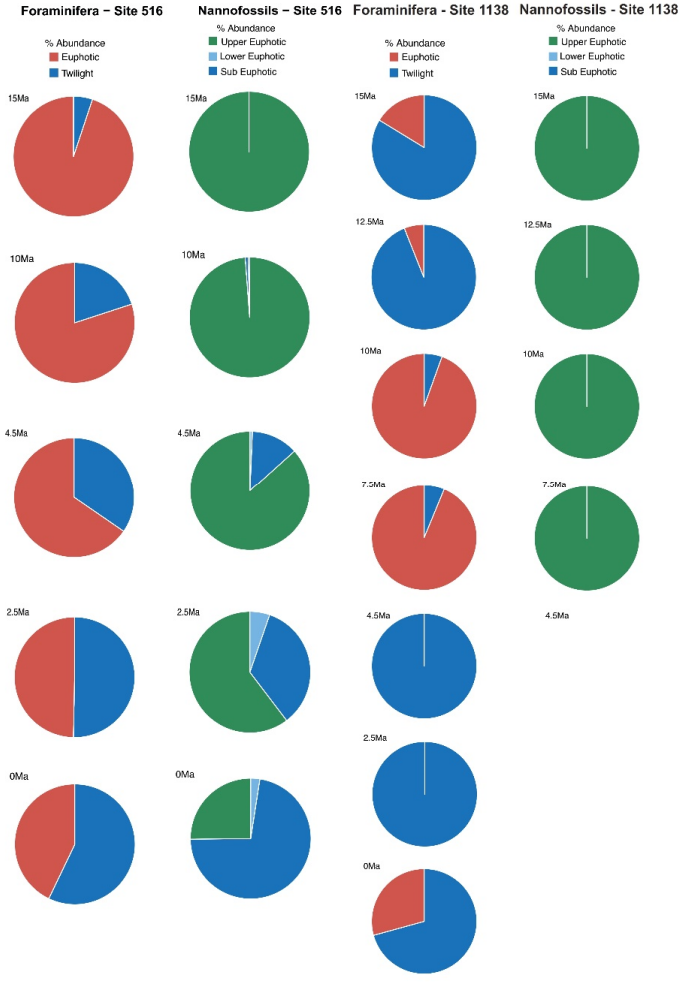

Figure 5. Foraminiferal and nannofossil ecogroup abundance at Site 516 and 1138.

https://doi.org/10.5194/bg-2021-230
Preprint. Discussion started: 18 October 2021

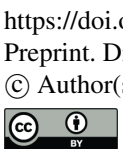

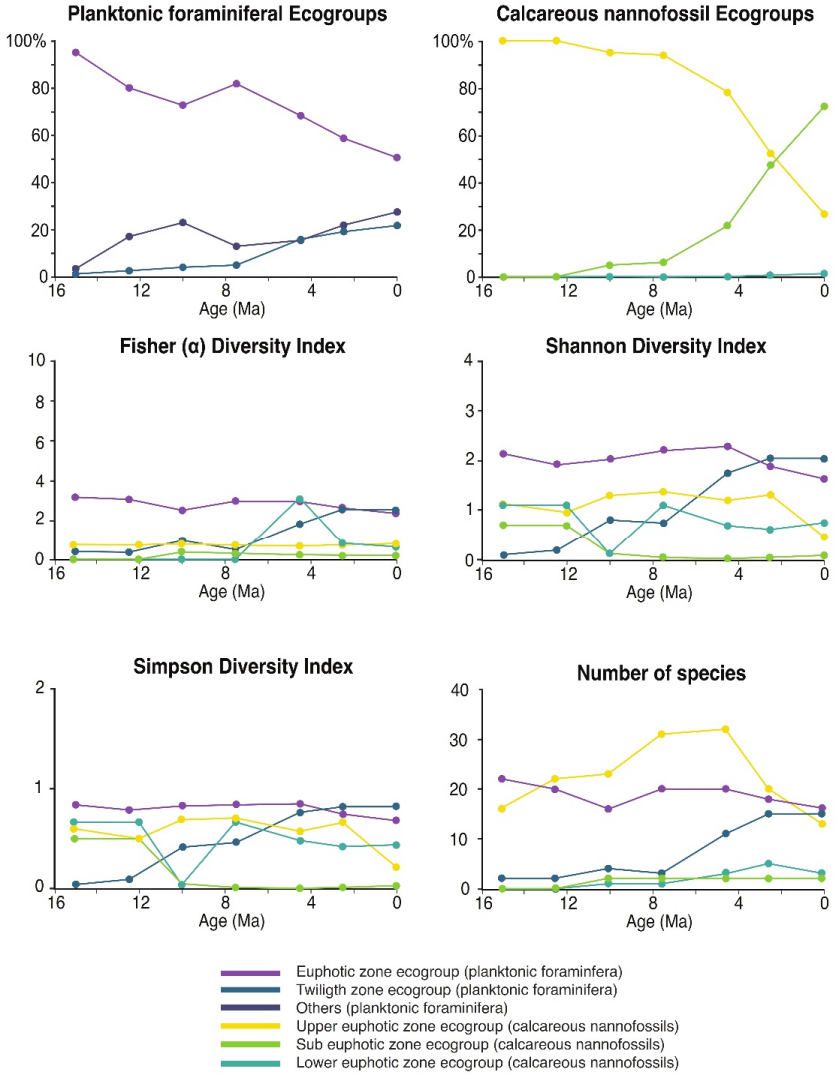

Figure 6. Planktonic foraminiferal and nannofossil ecogroups relative abundance and diversity indexes.

https://doi.org/10.5194/bg-2021-230
Preprint. Discussion started: 18 October 2021

3.2.3 Globorotaliids

With globorotaliids here we refer to the *Globorotalia merotumida-tumida* lineage composed by *G. merotumida*, *G. pleosiotumida*, *G. tumida* and *G. ungulata* (Kennett and Srinivasan, 1983). This group first appears with *Globorotalia plesiotumida* in our 10 Ma time slice at Site 871 (Fig. 7). At all the investigated low latitude sites, we find *G. tumida* by 4.5 Ma with abundances between 2-24% (Fig. 9). *Globorotalia plesiotumida* co-occurs with *G. tumida* only at Sites 872 and 242 corresponding to our 4.5 Ma time slice (Fig. 9; Fig. S9). In our records, *G. tumida* consistently displays oxygen isotope values between -1 to 0‰ (Figs. S3-S9), and an average depth habitat around 250 m, with a shallowest occurrence at 50 m and a deepest occurrence around 600 m (Fig. 1). Similar oxygen isotope values and depth habitat preference are recorded for *G. plesiotumida* and *G. ungulata* (Fig. 1 and Figs. S3-S9).

3.2.4 Globoconellids

In our records, *Globoconella miozea* is a dominant component of planktonic foraminiferal assemblage at Site 1138 at 15 Ma (65%) and occurs in moderate abundance at Site 516 (5%) (Fig. 7). The distribution of globoconellids appears restricted to southern high to mid-latitudes during the middle Miocene and the late Miocene to Pliocene. At Site 1138 globoconellids decrease in abundance through time, with *Globoconella panda* the only late Miocene species (<1%; with $\delta^{18}O$ of 3‰), followed only by *Globoconella inflata* in the Holocene (4.2%; with $\delta^{18}O$ of 3.5‰) (Fig. 11). On the contrary, at Site 516 globoconellids increase in abundance through time becoming a characteristic feature of the planktonic foraminifera assemblage as noted in previous studies of this area (Berggren, 1977; Norris et al., 1994) (Figs. 7-11). In the Holocene *G. inflata* is most abundant at mid-latitude Site 516 (22.7%; with $\delta^{18}O$ of 1‰), but also occurs in the subtropical (<0.5%; with $\delta^{18}O$ of 0.9‰) and subpolar Indian ocean (4.2%; with $\delta^{18}O$ of 3.5‰) (Fig. 11; Figs. S1-S3). Depth

https://doi.org/10.5194/bg-2021-230
Preprint. Discussion started: 18 October 2021

habitat reconstructions for the globoconellids show a deepening trend through time although less marked compared to those of other deep-dwelling groups considered in this study (Boscolo-Galazzo, Crichton et al., 2021; Fig. 1). At Site 516, the depth habitat is just above 200 m for middle Miocene *Globoconella miozea* ($\delta^{18}O$ 0.9‰), just below 200 m for late Miocene *G. conoidea* and *G. conomiozea* ($\delta^{18}O$ 1‰), and around 350 m for late Pliocene *Globoconella puncticulata* ($\delta^{18}O$ 1.6‰) the precursor of *G. inflata*, which shows a similar depth habitat at this site ($\delta^{18}O$ 1-1.2‰; Fig. S2), (Fig. 1). At Site 242 the average depth reconstruction for the Holocene *G. inflata* is of ~450 m ($\delta^{18}O$ 0.9‰; Fig. S3), similar to that of *T. crassaformis* and *T. truncatulinoides* (Boscolo-Galazzo, Crichton et al., 2021; Fig. 1).

4. Discussion

4.1 Evolution of a deep-plankton ecological niche linked to late Neogene cooling

We observe a trend of increasing ecological importance of deep-dwelling species in both calcareous nannofossil and foraminiferal communities from the late Miocene to Recent. The foraminiferal twilight zone ecogroup shows a marked increase in abundance and diversity at 7.5 Ma, at the same time as the first significant appearance of the sub-euphotic ecogroup within coccolithophore assemblages, and coinciding with a possible acceleration of global cooling (Cramer et al., 2011; Crichton et al., 2020). Fossil deep-dwelling coccoliths are dominated by one species, *Florisphaera profunda*, which is often very abundant in Plio-Pleistocene sediments. This makes our sub-euphotic ecogroup a low diversity – high abundance assemblage, whose origin significantly impacts the relative abundance balance between ecogroups, but with little change in diversity metrics towards the modern. Although there are morphological variants of *F. profunda* in the modern oceans, potentially representing sub-species or pseudo-cryptic species (Quinn et al., 2005), these are not distinguished in fossil assemblages and documenting their divergence times

https://doi.org/10.5194/bg-2021-230
Preprint. Discussion started: 18 October 2021

requires either further molecular genetic or detailed morphological analyses. The one clear signal in our diversity analyses is a late Miocene – early Pliocene peak in upper-euphotic species richness, followed by a marked decline through the late Pliocene to the Holocene. The late Miocene-Pliocene peak diversity is present in previous global compilations of total nannofossil diversity (Bown et al. 2004; Lowery et al. 2020), but here we show that this signal is driven by first a diversification and then progressive extinction almost entirely within upper-euphotic taxa.

Modern planktonic foraminifera evolved in two main diversification pulses in the middle Miocene (16-14 Ma) and during the late Miocene-Pliocene transition (6-4.5 Ma) (Kennett and Srinivasan, 1983; Kucera and Schönfeld, 2007). Our species abundance and diversity data show that this diversification was mostly driven by the origin of lineages of deep/subsurface dwelling species (Figs. 7-11 and Fig. 6). Diversity among euphotic zone species remained constant from the middle Miocene to the early Pliocene, then declined (Fig. 6). This pattern, similar to calcareous nannofossils, may explain early records pointing to a decrease in Pliocene to Recent planktonic foraminiferal diversity (Wei and Kennett, 1986).

The observed evolutionary patterns in planktonic foraminifera and coccolithophores can be explained by the development of environmental conditions favourable to deep living plankton

https://doi.org/10.5194/bg-2021-230
Preprint. Discussion started: 18 October 2021

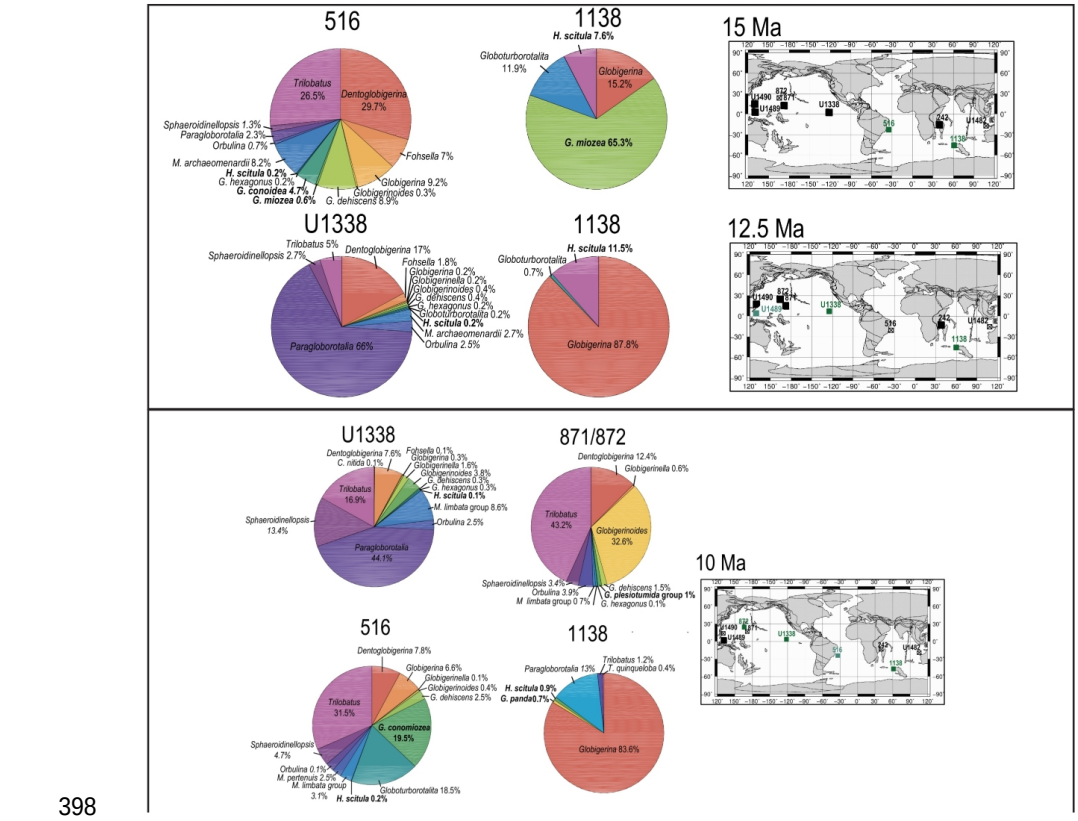

Figure 7. Abundance and biogeography of planktonic foraminiferal species at 15, 12.5, and 10 Ma. In the pie-charts twilight zone planktonic foraminiferal species are in bold. Sites where twilight zone planktonic foraminifera were found are highlighted in green in the maps. The crossed square symbol in the maps indicate that the time interval of interest was not recovered for a given site. Continental configuration follows: Ocean Drilling Stratigraphic Network (GEOMAR, Kiel, Germany).

https://doi.org/10.5194/bg-2021-230
Preprint. Discussion started: 18 October 2021

410 with cooling. For the deep-dwelling planktonic foraminifera, survival requires the availability of
411 food at depth, and with the exception of few species adapted to oxygen minimum zones (Davis et
412 al., 2021), the absence of severe oxygen depletion. In the published literature there is a general
413 tendency for planktonic foraminiferal $\delta^{18}O$ values to be tightly grouped during times of warm
414 climate, becoming more spread-out during cooling episodes, for instance the transition from mid-
415 to late Cretaceous (Ando et al., 2010) and early to middle Eocene (John et al., 2013). Because our
416 data are restricted to certain time slices and locations, we only capture a part of the overall pattern
417 for the Neogene, but other examples of depth-related evolution in the Neogene include the
418 *Fohsella peripheroronda – F. fohsi* lineage in the middle Miocene (Hodell and Vayavananda,
419 1993; Norris et al., 1993) and the appearance of various deep-dwelling digitate species in the Plio-
420 Pleistocene (Coxall et al., 2007).
421 Deep-dwelling coccolithophores, most notably *Florisphaera profunda*, require dissolved
422 macronutrients (N, P) and at least some degree of light penetration (Quinn et al., 2005; Poulton et
423 al., 2017). The requirement for light penetration to depth is most clearly shown by the absence
424 of *F. profunda* beneath high surface productivity regions where nutrients are not limited at depth
425 but light is rapidly attenuated by more abundant mixed layer microplankton (Beaufort et al., 1999).
426 For coccolithophores, the cooling-driven shift from nutrient recycling within to below the mixed
427 layer, may have provided the ecological driver for species to live in deeper, more nutrient-rich
428 waters, but, as mixed layer waters cleared, also allowed the irradiance necessary for photosynthesis
429 to penetrate to these new deeper habitats. Additionally, the capability of coccolithophores to absorb
430 carbon and nutrients from seawater under low light conditions (Godrjian et al., 2020) may have
431 also aided in the occupation of new deep water niches.

https://doi.org/10.5194/bg-2021-230
Preprint. Discussion started: 18 October 2021

Our model outputs from cGENIE is consistent with this interpretation, organic matter export (POC at 40 m in Fig. 12) reduced with cooling, suggesting an overall decrease in primary productivity at all 4 latitudinal bands considered in this study. Fewer particles in surface waters would have allowed greater light penetration (Fig. 12), at the same time, the model indicates enhanced organic matter delivery at >200 m with cooling. Greater organic matter delivery below the euphotic zone, suggests a deeper remineralization depth and increased dissolved nutrients availability at depth. This is most clearly shown in the modelled low and mid latitudes near-surface waters. Oxygen availability also increased, particularly below 100 m depth in low latitudes and further down the water column, below 200 m depth (Fig. 12).

Nonetheless, planktonic foraminifera and nannoplankton have distinct trophic statuses (zoo- versus phytoplankton), further coccolithophore species require light for their dominantly photosynthetic mode of life. In our data, such differences between the requirements of zoo- and phytoplankton deep-dwellers is clearly observed in the biogeographic patterns. Sub-euphotic coccolithophores are consistently more abundant in low nutrient sub-tropical locations (e.g. DSDP Site 242 and IODP Site U1482; Fig. 2). The end-member of this biogeographic difference is ODP Site 1138, in the Southern Ocean. Here, twilight foraminifera dominate most time intervals, presumably due to high export production. However, lower-euphotic and sub-euphotic coccolithophores are effectively excluded, due to turbid, high-productivity surface waters (Fig. 5). This pattern is also supported through a comparison of high to low productivity tropical sites in the Holocene – the Eastern Equatorial Pacific Site U1338 has abundant twilight foraminifera, but relatively low abundances of sub-euphotic taxa (Fig. 4), whereas the more oligotrophic Site U1482 (Fig. 2) has lower abundances of twilight foraminifera and higher abundances of sub-euphotic coccolithophores.

https://doi.org/10.5194/bg-2021-230
Preprint. Discussion started: 18 October 2021

Despite these ecological differences between zoo- and phytoplankton, there is a shared environmental driver for the evolution of deep-dwelling coccolithophores and planktonic foraminifera linking the evolution of deep-dwelling specialists in each group. Efficient near-surface recycling of organic carbon in past warm climates, such as the middle Miocene, precluded the occupation of the deep habitat for both groups by reducing both organic carbon transfer (food limitation for foraminifera and for foraminiferal prays such copepods) and light penetration (photosynthesis for coccolithophores) to depth. Global cooling since the middle Miocene (Kennett and Von der Borch, 1985; Kennett and Exon, 2004; Cramer et al., 2011; Zhang et al., 2014; Herbert et al., 2016; Sosdian et al., 2018; Super et al., 2020), however, led to a decreased export of organic matter and a deepening of the mean organic matter remineralization depth, which in turn favoured the evolution of deep water niches in planktonic foraminifera and nannoplankton via increased availability of organic matter, oxygen, and likely nutrients at depth, and clearing of surface waters.

4.2 Mechanisms of speciation of deep-dwelling planktonic foraminifera

The hirsutellids gave rise to a large late Neogene radiation among planktonic foraminifera, leading to the origin of modern phyletic groups such as the menardellids, globoconellids, truncorotaliids, and the globorotaliids of the *Globorotalia merotumida - tumida* lineage (Kennett and Srinivasan, 1983; Aze et al., 2011). The majority of the modern representatives of these groups are lower euphotic zone to twilight zone species. The hirsutellids originated about 18 Ma (Wade et al., 2011) from *Globorotalia zealandica* (Kennett and Srinivasan, 1983), the first representative of the group being *Hirsutella praescitula* (Kennett and Srinivasan, 1983; Aze et al., 2011). Extant hirsutellids include *H. scitula*, *H. hirsuta* and *H. theyeri*; genetic data available for *H. hirsuta* indicate a single genotype (Schiebel and Hembleben, 2017). Modern *H. scitula* and *H. hirsuta* are

https://doi.org/10.5194/bg-2021-230
Preprint. Discussion started: 18 October 2021

478 deep water forms. Depth habitat reconstructions show *H. scitula* at the greatest water depth
479 (Boscolo-Galazzo, Crichton et al., 2021; Fig. 1), consistent with it being reported to have a deeper
480 average depth habitat than *H. hirsuta* in the modern ocean (Birch et al., 2013; Stainbank et al.,
481 2019), where it feeds on suspended organic matter (Itou et al., 2001). *Hirsutella hirsuta* has been
482 reported to feed on dead diatoms and to predominantly live at depths around 250 m (Schiebel and
483 Hemleben, 2017), consistent with our habitat reconstructions placing *H. hirsuta* and other
484 hirsutellids shallower than *H. scitula*, between the bottom of the euphotic zone and the upper
485 twilight zone. Our depth habitat reconstruction for *H. scitula* at Site 516 for the 15 Ma time slice,
486 indicates an initial euphotic zone depth habitat preference for this species. By the 7.5 Ma time
487 slice, we find *H. scitula* at most of our low latitude sites, at depth comprised between 300-500 m
488 (Fig. 1). We suggest that the spread of *H. scitula* from high-mid latitudes towards the tropics after
489 the middle Miocene warmth (Figs. 7-11) tracks increasing availability of POC and oxygen at depth
490 (Boscolo-Galazzo, Crichton et al., 2021; Fig. 12), allowing this species to find food in deep tropical
491 twilight zone waters, profiting from a new ecological niche. We suggest that moving from a surface
492 to a deep-water habitat was for *H. scitula* an ecological innovation which allowed the species to
493 move outside its high-mid latitude areal, consistent with observations from the modern ocean
494 documenting *H. scitula* dwelling at progressively deeper depth from high to tropical latitudes
495 (Schiebel and Hemleben, 2017). The proceeding ocean cooling (and increasing efficiency of the
496 biological pump) explains the stepwise depth habitat increase of *H. scitula* through time at tropical
497 and subtropical sites (Fig.1): more food became available at increasingly greater depth in
498 association with improved oxygen availability (Fig. 12), allowing the species to expand its habitat
499

https://doi.org/10.5194/bg-2021-230
Preprint. Discussion started: 18 October 2021

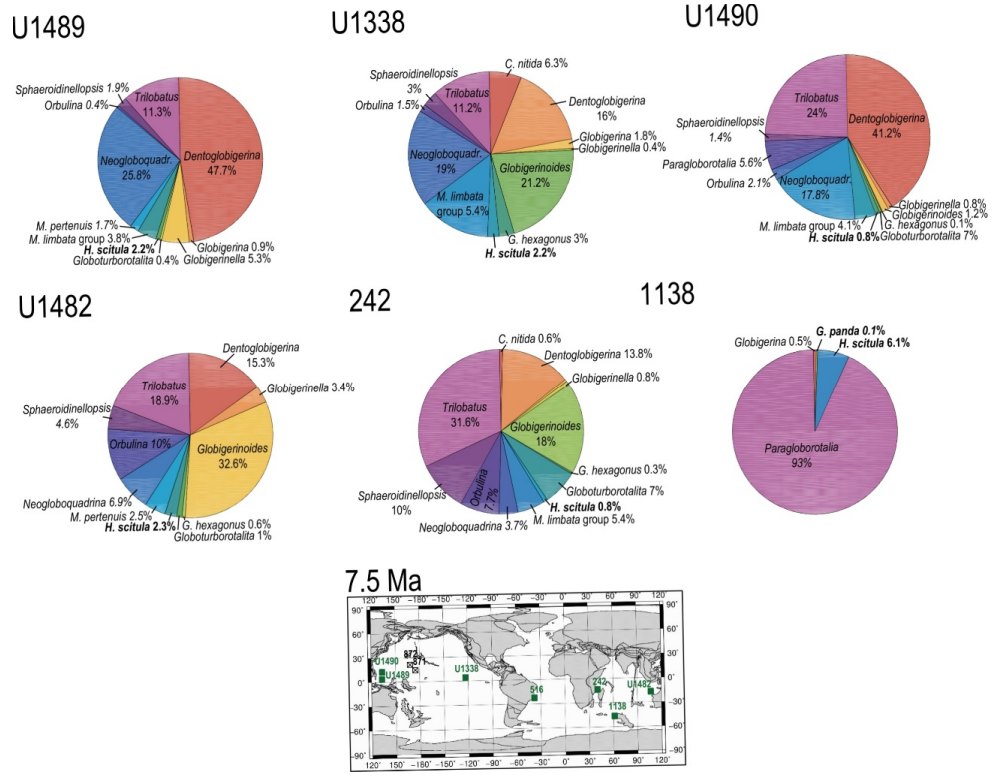

Figure 8. Abundance and biogeography of planktonic foraminiferal species at 7.5 Ma. In the pie-charts twilight zone planktonic foraminiferal species are in bold. Sites where twilight zone planktonic foraminifera were found are highlighted in green in the maps. The crossed square symbol in the maps indicate that the time interval of interest was not recovered for a given site. Continental configuration follows: Ocean Drilling Stratigraphic Network (GEOMAR, Kiel, Germany).

https://doi.org/10.5194/bg-2021-230
Preprint. Discussion started: 18 October 2021

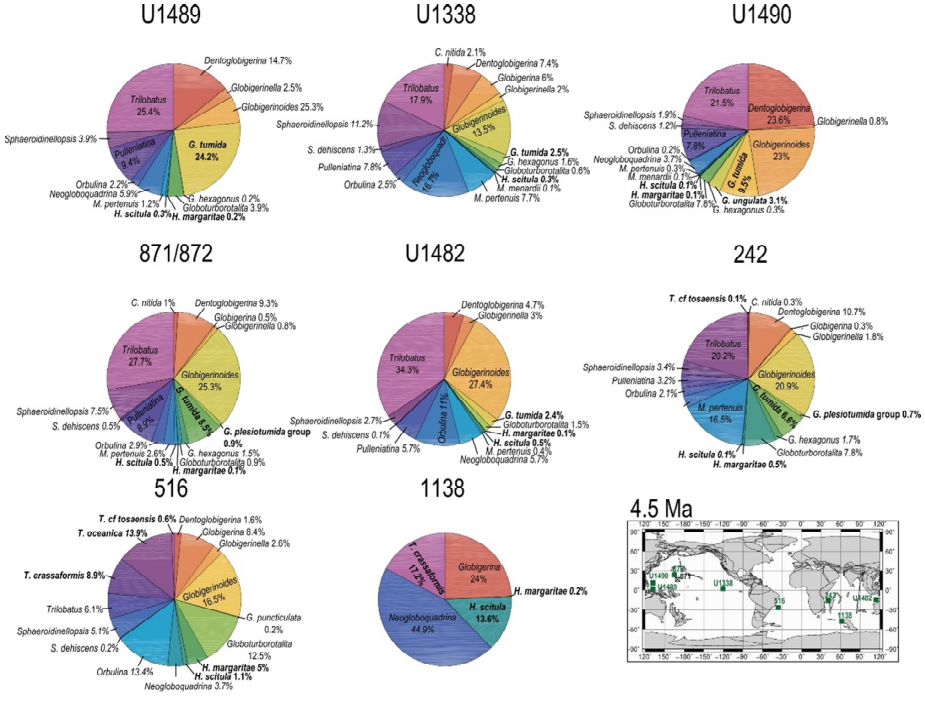

Figure 9. Abundance and biogeography of planktonic foraminiferal species at 4.5 Ma. In the pie-charts twilight zone planktonic foraminiferal species are in bold. Sites where twilight zone planktonic foraminifera were found are highlighted in green in the maps. The crossed square symbol in the maps indicate that the time interval of interest was not recovered for a given site. Continental configuration follows: Ocean Drilling Stratigraphic Network (GEOMAR, Kiel, Germany).

https://doi.org/10.5194/bg-2021-230
Preprint. Discussion started: 18 October 2021

523 vertically other than geographically. At low latitude sites this was accompanied by speciation, with
524 the appearance of *Hirsutella margaritae* and *H. theyeri* in the early Pliocene, and of *H. hirsuta* in
525 the Holocene. These new species display depth habitats shallower than *H. scitula* at their
526 appearance. Hence, we suggest that it was the occupation of a new deep water habitat in tropical
527 waters that triggered speciation from *H. scitula* through depth sympatry, i.e. genetic isolation
528 attained in the same area but at different depths (Weiner et al., 2012). Earlier studies on speciation
529 among planktonic foraminifera based on the fossil record, highlighted a predominance of
530 sympatric speciation, possibly linked to changes in ecology (Norris et al., 1993; Lazarus et al.,
531 1995; Pearson et al., 1997). This has more recently been supported by genetic analysis, which
532 reveals a consistent depth separation between intra-specific genotypes at a global scale, suggesting
533 that depth sympatry could be a universal mechanism generating diversity among microplankton
534 (Weiner et al., 2012).

535 Truncorotaliids start their evolutionary history at ~4.31 Ma (Raffi et al., 2020), when
536 *Truncorotalia crassaformis* splits from *Hirsutella cibaoensis* (Kennett and Srinivasan, 1983; Aze
537 et al., 2011), one of the first new species originating from *H. scitula* after its spread to low latitudes
538 (Kennett and Srinivasan, 1983). Our reconstructed geographic and temporal distribution for *T.*
539 *crassaformis* suggests that the early Pliocene split from the hirsutellids happened in cold subpolar
540 water. By the early Pliocene *Truncorotalia crassaformis* was an abundant component of the
541 subpolar assemblage at Site 1138 (>17%) and had already successfully spread to middle latitudes
542 (>8%) but does not occur in our low latitude samples (Fig.9).
543

https://doi.org/10.5194/bg-2021-230
Preprint. Discussion started: 18 October 2021

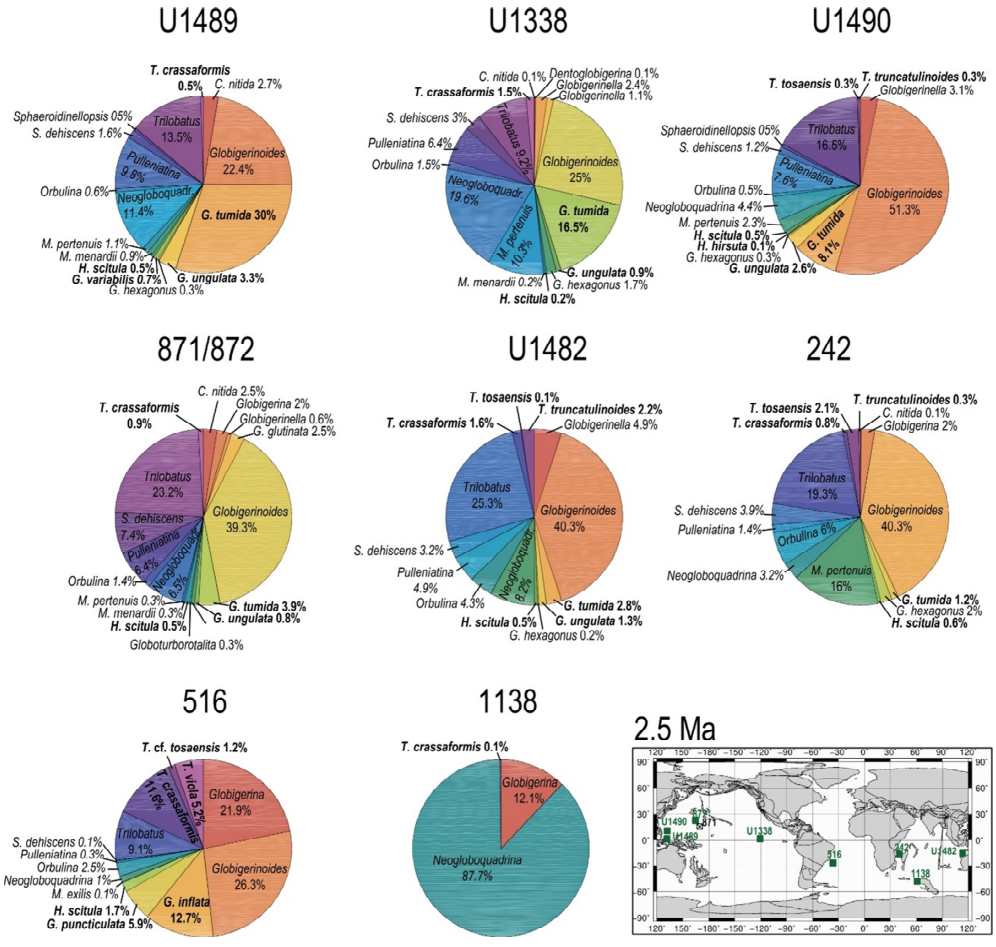

Figure 10. Abundance and biogeography of planktonic foraminiferal species at 2.5 Ma. In the pie-charts twilight zone planktonic foraminiferal species are in bold. Sites where twilight zone planktonic foraminifera were found are highlighted in green in the maps. The crossed square symbol in the maps indicate that the time interval of interest was not recovered for a given site. Continental configuration follows: Ocean Drilling Stratigraphic Network (GEOMAR, Kiel, Germany).

https://doi.org/10.5194/bg-2021-230
Preprint. Discussion started: 18 October 2021

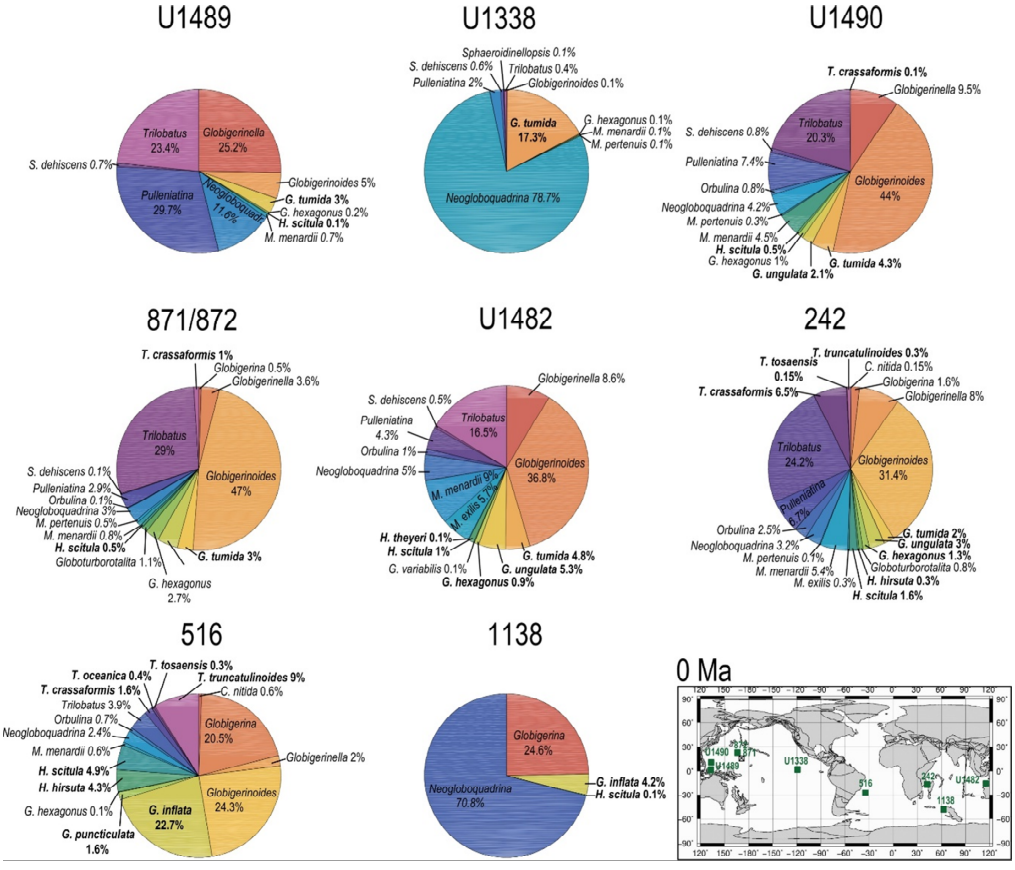

Figure 11. Abundance and biogeography of twilight zone planktonic foraminiferal species at 0 Ma. In the pie-charts twilight zone planktonic foraminiferal species are in bold. Sites where twilight zone planktonic foraminifera were found are highlighted in green in the maps. The crossed square symbol in the maps indicate that the time interval of interest was not recovered for a given site. Continental configuration follows: Ocean Drilling Stratigraphic Network (GEOMAR, Kiel, Germany).

https://doi.org/10.5194/bg-2021-230
Preprint. Discussion started: 18 October 2021

We suggest that the evolution of *Truncorotalia crassaformis* from the hirsutellids may have happened through allopatry, with low latitude population of *H. cibaoensis* becoming isolated from subpolar populations and eventually evolving into *T. crassaformis*. Similar to *H. scitula*, from subpolar latitudes, *Truncorotalia crassaformis* appears to have subsequently spread to lower latitudes occupying progressively deeper habitats (Fig. 1; Figs. 7-11), and originating numerous daughter species, some of which are intermediate morphospecies with limited geographic distributions no longer extant today (Lazarus et al., 1995). At Site 516 we find *Truncorotalia viola*, with lighter $\delta^{18}O$ and $\delta^{13}C$ values than *T. crassaformis* (Fig. S2), pointing to a clear ecological differentiation. Together with the marked morphological differentiation between the two, this suggests *T. viola* may have been a different biological species. *Truncorotalia truncatulinoides*, the most representative species of this group, appears to have originated from *T. crassaformis* at about 2.7 Ma in the tropical southwest Pacific, and subsequently spread in the global ocean (Dowsett, 1988; Lazarus et al., 1995). According to our reconstruction, depth sympatry associated with gradual morphological changes characterizes speciation among the truncorotaliids, as depth habitat deepening of the ancestor/precursor is clear in the transition *T. crassaformis-T. viola* and *T. crassaformis-T. tosaensis-T. truncatulinoides* in our record (Fig. 1). The possibility to colonize deeper water habitats may have led to progressive reproductive isolation between "deeper" and "shallower" populations of *T. crassaformis*, resulting in biological speciation. Depth sympatry as speciation mechanism for the truncorotaliids was already proposed by Lazarus et al. (1995) based on biogeography, but without a definitive test.

In the modern ocean the *Globorotalia merotumida-tumida* lineage is represented by *G. tumida* and *G. ungulata*, distributed in tropical to temperate regions. Genetic analysis has revealed that they are two distinct biological species with a single genotype each (Schiebel and Hemleben,

https://doi.org/10.5194/bg-2021-230
Preprint. Discussion started: 18 October 2021

584 2017). Little is known about the ecology of these two species, although *G. tumida* is known to
585 dwell in subsurface waters at the deep chlorophyll maximum (Schiebel and Hemleben, 2017).
586 According to the phylogeny of Aze et al. (2011), *Menardella menardii* gave rise to the
587 *Globorotalia merotumida-tumida* lineage around 9 Ma. However, *Menardella menardii* is absent
588 in our late Miocene samples while other menardellids such *Menardella limbata* and *M. pertenuis*
589 are common at several of our investigated middle latitudes to tropical sites. By 4.5 Ma,
590 *Globorotalia tumida* had evolved and is common at all of our low latitude sites (Fig. 9), while *M.*
591 *menardii* is extremely rare, occurring only at Sites U1338 and U1490 (0.1%), becoming more
592 common only by the Holocene. Based on this biogeographic pattern, we propose that the *G.*
593 *merotumida-tumida* lineage originated from a late Neogene menardellid, such for instance *M.*
594 *limbata* which is morphologically very similar to *G. merotumida*. Given that *G. plesiotumida* and
595 *G. tumida* display a deeper habitat (> 200 m) than *M. limbata* and other Miocene menardellids
596 (100-200 m), we suggest that such transition may have happened through depth sympatry in
597 tropical waters, with forms which remained reproductively isolated in the twilight zone generating
598 the *G. merotumida-tumida* lineage. Morphometric measurements on *M. limbata* and *G.*
599 *merotumida* shells are required to test for an evolutionary relationship between these two species.
600 According to our depth habitat reconstruction, *G. plesitumida* and *G. tumida* occupied a similar
601 depth habitat at 4.5 Ma, so it is not clear from our dataset which evolutionary mechanism may
602 have led to the origination of the latter from the first. Hull and Norris (2009) analyzed speciation
603 within this lineage and suggested that the evolution from *G. plesiotumida* to *G. tumida* happened
604 abruptly within 44 kyr. *Globorotalia ungulata*, appears in our record by the late Pliocene and often
605 display a habitat shallower than *G. tumida*, suggesting depth sympatry as the evolutionary
606 mechanism leading from *G. tumida* to *G. ungulata*. However, because depth habitat

https://doi.org/10.5194/bg-2021-230
Preprint. Discussion started: 18 October 2021

607 reconstructions for these two species are more variable and shallower than that of other twilight
608 zone species, more data are required to more conclusively infer speciation mechanisms.

609 The globoconellids originated in the late early Miocene (~17 Ma) with *Globoconella*
610 *miozea*, which is considered to descend directly from *Hirsutella praescitula* (Kennett and
611 Srinivasan, 1983; Norris et al., 1994; Aze et al., 2011). *Globoconella conoidea* originated in the
612 middle Miocene and, after the extinction of *G. miozea* at about 10 Ma, remained the only
613 representative of the globoconellids until the latest Miocene. At this time, the evolutionary
614 turnover within the group accelerated and a number of different morphospecies originate from *G.*
615 *conoidea* and go extinct very rapidly, until the appearance in the late Pliocene of *G. inflata* which
616 persists until today (Wei and Kennett, 1988; Wei, 1994; Aze et al., 2011). Compared to other
617 Neogene to Recent taxa, the globoconellids display a more restricted geographic distribution
618 throughout their evolutionary history. They tend to be common at mid latitude hydrographic fronts
619 (Schneider and Kennett, 1999; Schiebel and Hemleben, 2017; Lam and Leckie, 2020), except *G.*
620 *puncticulata* and *G. inflata*, which extend into low latitude regions (Norris et a., 1994). The
621 geographic distribution of globoconellids as shown here suggests that this group was already
622 specialized to live at hydrographic fronts in the middle Miocene, possibly feeding on
623 phytoplankton. Starting at ~5.5 Ma, cooling and the possibility to feed on sinking detritus in deeper
624 waters (Boscolo-Galazzo, Crichton et al., 2021) may have stimulated evolutionary turnover within
625 this otherwise rather static group. The closely spaced temporal succession of morphospecies at this
626 time may reflect ongoing evolutionary experiments in an attempt to profit from new ecological
627 possibilities opening up at depth and outside the area of the group. The depth habitat
628 reconstructions for *G. puncticulata* and *G. inflata* suggests that from the Pliocene this group started

https://doi.org/10.5194/bg-2021-230
Preprint. Discussion started: 18 October 2021

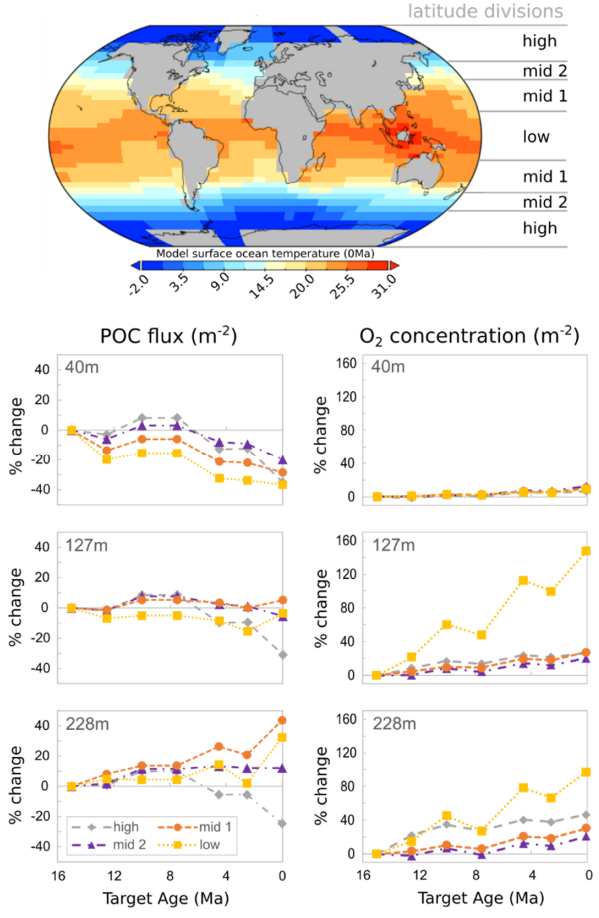

Figure 12. cGENIE model output for changes in Particulate Organic Carbon (POC) flux, and dissolved Oxygen in near-surface ocean waters from the middle Miocene to Present, with a temperature-dependent biological carbon pump. Inset map shows the modelled Present surface ocean temperatures. Depths are the middle of cGENIE's top three ocean layers.

https://doi.org/10.5194/bg-2021-230
Preprint. Discussion started: 18 October 2021

635 to progressively adapt to greater depths, consistent with the distinctive change in morphology
636 between G. sphericomiozea (and other Miocene globoconellids) and its Pliocene descendants *G.*
637 *puncticulata* and *G. inflata* (Kennett and Srinivasan, 1983). We suggest that an evolutionary
638 transition began with the morphospecies *G. puncticulata*, transitional between *G. sphericomiozea*
639 and *G. inflata* and led to the late Pliocene speciation of *G. inflata*. It is not clear from our data
640 whether depth sympatry or allopatry allowed the speciation of *G. inflata*, as *G. puncticulata* and
641 *G. inflata* show similar depth habitat in our record. It may have been a combination of the two,
642 given *G. inflata* genotypes display a characteristic allopatric distribution in the ocean (Morard et
643 al., 2011).

644 Our data indicate that combining stable isotopes and model-derived water column temperature
645 is a promising approach to quantify the depth habitat of extinct planktonic foraminiferal species.
646 When combined with abundance and biogeographic data, depth habitat reconstructions offer
647 insights into speciation mechanisms not resolvable with the use of one technique alone (e.g., stable
648 isotopes). Our reconstructions indicate that both allopatry and depth sympatry played a role in the
649 origin of modern deep-dwelling planktonic foraminiferal species. Both allopatry and depth
650 sympatry appear to have been involved with the cladogenesis of the truncorotaliid and the
651 globorotaliid lineages, while depth sympatry seems to be mostly involved for intra-lineage
652 speciation.

653 **5. Conclusions**

654 Our global abundance and biogeographic data combined with our depth habitat
655 reconstructions allow us to piece together the environmental drivers behind speciation in two of
656 the most extensively studied group of pelagic microfossils, planktonic foraminifera and calcareous
657 nannofossils over the last 15 million years. The evolution of the new Neogene deep-water lineages

https://doi.org/10.5194/bg-2021-230
Preprint. Discussion started: 18 October 2021

of the hirsutellids, globorotaliids, globoconellids and truncorotaliids, and of nannoplankton lower-euphotic zone and sub-euphotic zone species, resulted in the vertical stratification of species seen in the modern ocean, in particular at low latitudes. For planktonic foraminifera such vertical stratification of species, hundreds of meters below the surface, originated through depth sympatry as well as cladogenesis of new lineages via both sympatry and allopatry.

Our study places the evolution of modern plankton groups in the context of large scale changes in ocean macroecology driven by the global climate dynamics of the past fifteen million years. The late Miocene to present evolutionary history of planktonic foraminifera and nannoplankton was linked, wherein increased efficiency of the biological pump with cooling since the middle Miocene was a shared evolutionary driver. Lower rates of organic matter remineralization in the upper part of the water column allowed the creation of new ecological niches in deep waters, by increasing food delivery and oxygen at depth for heterotrophic planktonic foraminifera, and by clearing surface waters and augmenting the concentration of macronutrients at depth for nannoplankton.

https://doi.org/10.5194/bg-2021-230
Preprint. Discussion started: 18 October 2021

673 **Data availability:** All data associated with this article are available in the Supplement or have
674 been previously published. The code is tagged as v0.9.18 and is available at DOI:
675 10.5281/zenodo.4469673 and at: DOI: 10.5281/zenodo.4469678.
676
677 **Author contributions:**
678 Conceptualization, F.B.G. and P.N.P.; investigation, F.B.G. (planktonic foraminifera) and A.J.
679 (nannofossils); software, K.A.C.; writing–original draft, F.B.G.; writing–review and editing,
680 F.B.G., A.J., T.D.J, K.A.C., P.N.P., B.S.W.; visualization, F.B.G., A.J., K.A.C.; project
681 administration and funding acquisition, P.N.P. and B.S.W.
682
683 **Competing interests:**
684 The authors declare that they have no conflict of interest.
685 **Acknowledgements:**
686 Supported by Natural Environment Research Council (NERC) grant NE/N001621/1 to P.N.P.
687 (F.B.G. and K.A.C.), NERC grant NE/P019013/1 to B.W and NERC grant NE/P016375/1 to
688 participate in IODP Expedition 363 (P.N.P.). A.J. was founded by a CENTA Doctoral Training
689 Programme as part of NERC grant: NE/L002493/1 to T.D.J. We thank Ian Hall for becoming
690 acting Principal Investigator in the later stages of the grant and Jamie Wilson for insightful
691 discussions.
692

693 **References**

694 Ando, A., Huber, B.T., and MacLeod, K.G.: Depth-habitat reorganization of planktonic
695 foraminifera across the Albian/Cenomanian boundary, Paleobiology, 36, 357-373, 2010.

https://doi.org/10.5194/bg-2021-230
Preprint. Discussion started: 18 October 2021

696 Aze, T., Ezard, T.H.G., Purvis, A., Coxall, H.K., Stewart, D.R.M., Wade, B.S., and Pearson, P.N.:
697 A phylogeny of Cenozoic macroperforate planktonic foraminifera from fossil data, Biological
698 Reviews, 86, 900–927, 2011.

699 Bergen, J.A., de Kaenel, E., Blair, S.A., Boesiger, T.M., and Browning, E.: Oligocene-Pliocene
700 taxonomy and stratigraphy of the genus Sphenolithus in the circum North Atlantic Basin: Gulf of
701 Mexico and ODP Leg 154, J. Nannoplankt. Res. 37, 77–112, 2017.

702 Berggren, W.A.: Late Neogene planktonic foraminiferal biostratigraphy of the Rio Grande Rise
703 (SouthAtlantic). Mar. Micropaleontol., 2, 265-313, 1977.

704 Birch, H., Coxall, H.K., Pearson, P.N., Kroon, D., and O'Regan, M.: Planktonic foraminifera
705 stable isotopes and water column structure: Disentangling ecological signals, Marine
706 Micropaleontology, 101, 127–145, 2013.

707 Blair, S.A., Bergen, J.A., de Kaenel, E., Browning, E., and Boesiger, T.M.: Upper Miocene-Lower
708 Pliocene taxonomy and stratigraphy in the circum North Atlantic Basin: radiation and extinction
709 of Amauroliths, Ceratoliths and the D. quinqueramus lineage, Journal of Nannoplankton Research.
710 37, 113–144, 2017

711 Boesiger, T.M., de Kaenel, E., Bergen, J.A., Browning, E., and Blair, S.A.: Oligocene to
712 Pleistocene taxonomy and stratigraphy of the genus Helicosphaera and other placolith taxa in the
713 circum North Atlantic Basin, Journal of Nannoplankton Research. 37, 145–175, 2017.

714 Boscolo-Galazzo, F., Crichton, K.A., Ridgwell, A., Mawbey, E.M., Wade, B.S., and Pearson P.N.:
715 Temperature controls carbon cycling and biological evolution in the ocean twilight zone, Science,
716 371, 1148–1152, 2021.

https://doi.org/10.5194/bg-2021-230
Preprint. Discussion started: 18 October 2021

717 Bown, P.R., and Young, J.R, Techniques. In: P.R. Bown (Ed.). Calcareous Nannofossil
718 Biostratigraphy, British Micropalaeontological Society Publications Series/Kluwer Academic,
719 London, 16–28 pp., 1998.

720 Bown, P.R., Lees, J.A., and Young, J.R.: Calcareous nannoplankton evolution and diversity
721 through time. In: H.R. Thierstein and J.R. Young (Editors), Coccolithophores: From Molecular
722 Processes to Global Impact. Springer, Berlin, 481-508, 2004.

723 Browning, E., de Kaenel, E., Bergen, J.A., Blair, S.A., and Boesiger, T.M.: Oligocene-Pliocene
724 taxonomy and stratigraphy of the genus *Sphenolithus* in the circum North Atlantic Basin: Gulf of
725 Mexico and ODP Leg 154, Journal of Nannoplankton Research, 37, 77–112, 2017.

726 Ciummelli, M., Raffi, I., and Backman, J.: Biostratigraphy and evolution of Miocene Discoaster
727 spp. from IODP Site U1338 in the equatorial Pacific Ocean, J. Micropalaeontology, 36,
728 jmpaleo2015-034, 2016.

729 Coxall, H.K., Wilson, P.A., Pearson, P.N., and Sexton, P.F.: Iterative evolution of digitate
730 planktonic foraminifera. Paleobiology, 33, 495–516, 2007.

731 Cramer, B.S., Miller, K.G., Barrett P.J., and Wright, J.D.: Late Cretaceous–Neogene trends in deep
732 ocean temperature and continental ice volume: Reconciling records of benthic foraminiferal
733 geochemistry (d18O and Mg/Ca) with sea level history. J. Geophys. Res., 116, C12023, 2011.

734 Crichton K.A., Ridgwell A., Lunt D.J., Farnsworth A., and Pearson P.N.: Data-constrained
735 assessment of ocean circulation changes since the middle Miocene in an Earth system model. Clim.
736 Past https://doi.org/10.5194/cp-2019-151, 2020.

https://doi.org/10.5194/bg-2021-230
Preprint. Discussion started: 18 October 2021

737 Crichton, K.A., Wilson, J.D., Ridgwell, A., and Pearson P.N.: Calibration of key temperature-
738 dependent ocean microbial processes in the cgenie.muffin Earth system model, Geosciences
739 Model Development, 14, 125–149, 2021.

740 de Kaenel, E., Bergen, J.A., Browning, E., Blair, S.A., and Boesiger, T.M.: Uppermost Oligocene
741 to Middle Miocene Discoaster and Catinaster taxonomy and stratigraphy in the circum North
742 Atlantic Basin: Gulf of Mexico and ODP Leg 154, Journal of Nannoplankton Research, 37, 77–
743 112, 2017.

744 De Vargas, Renaud, C.S., Hilbrecht, H., and Pawlowski, J.: Pleistocene adaptive radiation in
745 Globorotalia truncatulinoides: genetic, morphologic, and environmental evidence, Paleobiology,
746 27, 104–125, 2001.

747 Davis, C.V., Wishner, K., Renema, W., and Hull, P.M.,: Vertical distribution of planktic
748 foraminifera through an oxygen minimum zone: how assemblages and test morphology reflect
749 oxygen concentrations, Biogeosciences, 18, 977–992, 2021.

750 Dowsett, H.J.: Diachrony of late Neogene microfossils in the Southwest Pacific Ocean: application
751 of the graphic correlation method, Paleoceanography, 3, 209-222, 1988.

752 Ezard, T.H.G., Aze, T., Pearson, P.N., and Purvis, A.: Interplay Between Changing Climate and
753 Species' Ecology Drives Macroevolutionary Dynamics, Science, 332, 349-351, 2011.

754 Fraass, A.J., Kelly, D.C., and Peters, S.E.: Macroevolutionary History of the Planktic
755 Foraminifera, Annu. Rev. Earth Planet. Sci., 431, 39–66, 2015.

https://doi.org/10.5194/bg-2021-230
Preprint. Discussion started: 18 October 2021

Godrijan, J., Drapeau, D., and Balch, W.M.: Mixotrophic uptake of organic compounds by coccolithophores, Limnology and Oceanography 00, 1–12, 2020.

Gibbs, S.J., Bown, P.R., Ward, B.A., Alvarez, S.A., Kim, H., Archontikis, O.A., Sauterey, B., Poulton, A.J., Wilson, J., and Ridgwell, A.: Algal plankton turn to hunting to survive and recover from end-Cretaceous impact darkness, Sci. Adv. 6, eabc9123, 2020.

Greco, M., Jonkers, L., Kretschmer, K., Bijma, J., and Kucera, M.: Depth habitat of the planktonic foraminifera Neogloboquadrina pachyderma in the northern high latitudes explained by sea-ice and chlorophyll concentrations, Biogeosciences, 16, 3425–3437, 2019.

Hammer, Ø., Harper, D.A.T., and Ryan, P.D.: PAST: Paleontological Statistics Software Package for Education and Data Analysis, Palaeontologia Electronica 4, 9 pp., 2001.

Henderiks, J., Bartol, M., Pige, N., Karatsolis, B.-T., and Lougheed, B.C.: Shifts in phytoplankton composition and stepwise climate change during the middle Miocene, Paleoceanography and Paleoclimatology, 35, e2020PA003915, 2020.

Herbert, T.D., Lawrence, K.T., Tzanova, A., Peterson, L.C., Caballero-Gill, R., and Kelly, C.S.: Late Miocene global cooling and the rise of modern ecosystems. Nature Geoscience, 9, 843–847, 2016.

Hodell, D.A. and Vayavananda, A.: Middle Miocene paleoceanography of the western equatorial Pacific (DSDP Site 289) and the evolution of Globorotalia (Fohsella), Marine Micropaleontology, 22, 279–310, 1993.

https://doi.org/10.5194/bg-2021-230
Preprint. Discussion started: 18 October 2021

775 Hull P.M., and Norris R.D.: Evidence for abrupt speciation in a classic case of gradual evolution,
776 PNAS, 106, 21224–21229, 2009.

777 Hull, P. M., Osborn, K. J., Norris, R. D., and Robison, B. H.: Seasonality and depth distribution
778 of a mesopelagic foraminifer, Hastigerinella digitata, Monterey Bay, California, Limnol.
779 Oceanogr., 56, 562–576, 2011.

780 Itou, M., Ono, T., Olba, T., and Noriki, S.: Isotopic composition and morphology of living
781 Globoborotalia scitula: a new proxy of sub-intermediate ocean carbonate chemistry? Marine
782 Micropaleontology, 42, 189-210, 2001.

783 John, E.H., P.N. Pearson, H.K. Coxall, H. Birch, B.S. Wade, and Foster G.L.: Warm ocean
784 processes and carbon cycling in the Eocene, Philos. Trans. R. Soc. A, doi:10.1098/rsta.2013.0099,
785 2013.

786 Jones, A.P., Dunkley Jones, T., Coxall, H., Pearson, P.N., Nala, D. and Hoggett, H.: Low-latitude
787 calcareous nannofossil response in the Indo-Pacific Warm Pool across the Eocene–Oligocene
788 Transition of Java, Indonesia. Paleoceanography and Paleoclimatology, 34, 1–15, 2019

789 Jonkers, L., and Kucera, M.: Global analysis of seasonality in the shell flux of extant planktonic
790 Foraminifera, Biogeosciences, 12, 2207–2226, 2015.

791 Kennett, J.P., and Srinivasan, M.S.: Neogene Planktonic Foraminifera. Hutchinson Ross
792 Publishing Co., Stroudsburg, Pennsylvania, 1-265 pp, 1983.

https://doi.org/10.5194/bg-2021-230
Preprint. Discussion started: 18 October 2021

793 Kennett, J.P., and Von der Borch, C.C.: Southwest Pacific Cenozoic Paleoceanography. In
794 Kennett, J.P., von der Borch, C.C., et al., Initial Reports of the Deep Sea Drilling Project, 90:
795 Washington, DC (U.S. Government Printing Office), 1493–1517, 1986.

796 Kennett, J.P., and Exon, N.F.: Palaeoceanographic Evolution of the Tasmanian Seaway and its
797 Climatic Implications, In: Exon, N.F., Kennett, J.P., and Malone, M.J. (Eds.), The Cenozoic
798 Southern Ocean: Tectonics, Sedimentation, and Climate Change between Australia and
799 Antarctica. Geophysical Monograph, 151, 345–367, 2004.

800 Kim S.-T., and O'Neil J.R.: Equilibrium and non-equilibrium oxygen isotope effects in synthetic
801 carbonates. Geochim. Cosmochim. Acta, 61, 3461–3475, 1997.

802 Kucera, M., and Schonfeld, J.: The origin of modern oceanic foraminiferal faunas and Neogene
803 climate change, in Williams, M., Haywood, A.M., Gregory, F.J. and Schmidt, D.N. (eds) Deep-
804 Time Perspectives on Climate Change: Marrying the Signal from Computer Models and Biological
805 Proxies. The Micropalaeontological Society, Special Publications, The Geological Society,
806 London, 409–425, 2007.

807 Lam A.R., and Leckie R.M.: Late Neogene and Quaternary diversity and taxonomy of subtropical
808 to temperate planktic foraminifera across the Kuroshio Current Extension, northwest Pacific
809 Ocean, Micropaleontology, 66, 177–268, 2020.

810 Lazarus, D.B., Hilbrecht, H., Spencer-Cervato, C. and Thierstein, H.: Sympatric speciation and
811 phyletic change in Globorotalia truncatulinoides, Paleobiology, 21, 28–51, 1995.

https://doi.org/10.5194/bg-2021-230
Preprint. Discussion started: 18 October 2021

812 Lowery, C.M., Bown, P.R., Fraass, A.J. and Hull, P.M.,: Ecological Response of Plankton to
813 Environmental Change: Thresholds for Extinction, Annual Review of Earth and Planetary
814 Sciences, 48, 403-429, 2020.

815 Meilland, J., Siccha, M., Weinkauf, M. F. G., Jonkers, L., Morard, R., Baranowski, U., Baumeister,
816 A., Bertlich, J., Brummer, G. J., Debray, P., Fritz-Endres, T., Groeneveld, J., Magerl, L., Munz,
817 P., Rillo, M. C., Schmidt, C., Takagi, H., Theara, G., and Kucera, M.: Highly replicated sampling
818 reveals no diurnal vertical migration but stable species-specific vertical habitats in planktonic
819 foraminifera, J. Plank. Res., 41, 127–141, 2019.

820 Norris, R., D.: Pelagic Species Diversity, Biogeography, and Evolution, Paleobiology, 26, 236-
821 258, 2000.

822 Norris, R.D., and Corfield, R.M.: Evolutionary ecology of Globorotalia (Globoconella) (planktic
823 foraminifera), Marine Micropaleontology, 23, 121–145, 1994.

824 Norris, R.D., Corfield, R.M. and Cartlidge, J.E.: Evolution of depth ecology in the planktic
825 foraminifera lineage Globorotalia (Fohsella). Geology, 21, 975–978, 1993.

826 Norris, R. D., Kirtland Turner, S., Hull, P. M., and Ridgwell, A.: Marine Ecosystem Responses to
827 Cenozoic Global Change, Science, 341, 492-498, 2013.

828 Morard, R., Quillevere, F., Douady, C.J., De Vargas, C., De Garidel-Thoron, T., and Escarguel,
829 G.: Worldwide Genotyping in the Planktonic Foraminifer Globoconella inflata: Implications for
830 Life History and Paleoceanography, PLoS ONE 6(10): e26665, 2011.

https://doi.org/10.5194/bg-2021-230
Preprint. Discussion started: 18 October 2021

831 Pearson, P.N., and Coxall, K.H.: Origin of the Eocene planktonic foraminifer Hantkenina by
832 gradual evolution, Palaeontology 57, 243–267, 2012.

833 Pearson, P.N., N.J. Shackleton, and Hall M.A.: Stable isotopic evidence for the sympatric
834 divergence of Globigerinoides trilobus and Orbulina uniriersa (planktonic foraminifera), Journal
835 of the Geological Society, 154, 295-302, 1997.

836 Quillevere F., Norris R.D., Moussa I., and Berggren W.A.: Role of photosymbiosis and
837 biogeography in the diversification of early Paleogene acarininids (planktonic foraminifera),
838 Paleobiology, 27, 311–326, 2001.

839 Quinn, P.S., Cortés, M.Y. and Bollmann, J.: Morphological variation in the deep ocean-dwelling
840 coccolithophore Florisphaera profunda (Haptophyta), European Journal of Phycology, 40, 123-
841 133, 2005.

842 Raffi, I., Wade, B.S., Pälike, H., Beu, A.G., Cooper, R., Crundwell, M.P., Krijgsman, W., Moore,
843 T., Raine, I., Sardella, R., and Vernyhorova, Y.V.: Chapter 29 - The Neogene Period, Editor(s):
844 Felix M. Gradstein, James G. Ogg, Mark D. Schmitz, Gabi M. Ogg, Geologic Time Scale 2020,
845 Elsevier, 1141-1215 pp., 2020

846 Rebotim, A., Voelker, A. H. L., Jonkers, L., Waniek, J. J., Meggers, H., Schiebel, R., Fraile, I.,
847 Schulz, M., and Kucera, M.: Factors controlling the depth habitat of planktonic foraminifera in the
848 subtropical eastern North Atlantic, Biogeosciences, 14, 827–859, 2017.

849 Schiebel, R., and Hemleben, C.: Planktic Foraminifers in the Modern Ocean, Springer-Verlag,
850 Berlin Heidelberg, 2017.

https://doi.org/10.5194/bg-2021-230
Preprint. Discussion started: 18 October 2021

851 Schiebel R., Smart S.M., Jentzen A., Jonkers L., Morard R., Meilland J., Michel E., Coxall H.K.,
852 Hull P.M., De Garidel-Thoron T., Aze T., Quillévéré F., Ren H., Sigman D.M., Vonhof H.B.,
853 Martínez-García A., Kucera M., Bijma J., Spero H.J., and Haug G.H., Advances in planktonic
854 foraminifer research: New perspectives for paleoceanography, Revue de micropaléontologie, 61,
855 113–138, 2018.

856 Schneider, C., and Kennett, J.: Segregation and speciation in the Neogene planktonic foraminiferal
857 clade Globoconella, Paleobiology, 25, 383-395, 1999.

858 Sosdian, S.M., Greenop, R., Hain, M.P., Foster, G.L., Pearson, P.N., and Lear, C.H.: Constraining
859 the evolution of Neogene ocean carbonate chemistry using the boron isotope pH proxy, Earth and
860 Planetary Science Letters, 498, 362–376, 2018.

861 Stainbank, S., Kroon, D., Ruggeberg, A., Raddatz, J., de Leau, E.S., Zhang, M., and Spezzaferri,
862 S.: Controls on planktonic foraminifera apparent calcification depths for the northern equatorial
863 Indian Ocean, PLoS ONE, 14, e0222299, 2019.

864 Styzen, M.J.. Cascading counts of nannofossil abundance, Journal of Nannoplankton Research,
865 19, 49, 1997.

866 Super, J.R., Thomas, E., Pagani, M., Huber, M., O'Brien, C.L., and Hull, P. M.: Miocene evolution
867 of North Atlantic Sea surface temperature. Paleoceanography and Paleoclimatology, 35,
868 e2019PA003748, 2020.

869 Wade, B.S., Pearson, P.N. Berggren, W.A. and Palike, H.: Review and revision of Cenozoic
870 tropical planktonic foraminiferal biostratigraphy and calibration to the geomagnetic polarity and
871 astronomical time scale, Earth-Science Reviews, 104, 111–142, 2011.

https://doi.org/10.5194/bg-2021-230
Preprint. Discussion started: 18 October 2021

872 Wade, B.S., Pearson, P.N., Olsson, R.K., Fraass, A. Leckie, R.M. and Hemleben, Ch.: Taxonomy,
873 biostratigraphy, and phylogeny of Oligocene and lower Miocene Dentoglobigerina and
874 Globoquadrina, in Wade, B.S., Olsson, R.K., Pearson, P.N., Huber, B.T. and Berggren, W.A.,
875 Atlas of Oligocene Planktonic Foraminifera, Cushman Foundation of Foraminiferal Research,
876 Special Publication, No. 46, p. 331-384, 2018.

877 Wei, K.Y.: Stratophenetic tracing of phylogeny using SIMCA pattern recognition technique: A
878 case study of the late Neogene planktic foraminifera Globoconella clade, Paleobiology, 20, 52-65,
879 1994.

880 Wei, K.Y., and Kennett, J.P.: Taxonomic evolution of Neogene planktonic foraminifera and
881 paleoceanographic relations, Paleoceanography, 1, 67-84, 1986.

882 Wei, K.Y., and Kennett, J.: Phyletic gradualism and punctuated equilibrium in the late Neogene
883 planktonic foraminiferal clade Globoconella, Paleobiology, 14, 345-363, 1988.

884 Weiner, A., Aurahs, R., Kurasawa, A., Kitazato, H., and Kucera, M.: Vertical niche partitioning
885 between cryptic sibling species of a cosmopolitan marine planktonic protest, Mol. Ecol., 21, 4063–
886 4073, 2012.

887 Woodhouse, A., Jackson, S.L., Jamieson, R.A., Newton, R.J., Sexton, P.F., and Aze, T.: Adaptive
888 ecological niche migration does not negate extinction susceptibility. Scientific Reports, 11, 15411,
889 2021.

890 Young, J.R., Bergen, J.A., Bown, P.R., Burnett, J.A., Fiorentino, A., Jordan, R.W., Kleijne, A.,
891 van Niel, B.E., Romein, A.J.T. and Von Salis, K.: Guidelines for coccolith and calcareous
892 nannofossil terminology, Palaeontology, 40, 875–912, 1997.

https://doi.org/10.5194/bg-2021-230
Preprint. Discussion started: 18 October 2021

893 Zhang, Y.G., Pagani, M., Liu Z.: A 12-Million-Year Temperature History of the Tropical Pacific
894 Ocean, Science, 344, 84-87, 2014.

895 Zenodo DOI: 10.5281/zenodo.4469673.

896 Zenodo DOI: 10.5281/zenodo.4469678.